ISI MITIGATION TECHNIQUES IN MOLECULAR COMMUNICATION

by

Burcu Tepekule

B.S., Electrical and Electronics Engineering, Boğaziçi University, 2013

Submitted to the Institute for Graduate Studies in
Science and Engineering in partial fulfillment of
the requirements for the degree of
Master of Science

Graduate Program in Electrical and Electronics Engineering
Boğaziçi University

2015

ACKNOWLEDGEMENTS

I would like to express my gratitude to people who have contributed to this work and have made this thesis possible.

I would like to thank my family first. I have always felt their endless support with me, even though they were far away. I am mostly greatful to my mom, my little brother and my father. I now they will always stand by me and I cannot describe how lucky I am to have such a family.

I couldn't have done this work without the support of my supervisor, Assoc. Prof. Ali Emre Pusane. I cannot describe how lucky I am to find an opportunity to be the student of such a great mentor, who supported me in every dimension of my life. His smart ideas, his patience, and most of it all, his faith in me made me the researcher I am now, and made this thesis possible. It was, and it still will be a great pleasure to work with him. I would also like to thank Prof. Tuna Tuğcu, whose support and valuable contributions were always with me throughout this study.

There are some dearest people that I would like to mention here. I am thankful to Emre İşeri for his precious friendship since 2009. He was my best friend throughout my time in Bogaziçi, and I know I can count on him for the rest of my life. I am such a lucky person to work in the same lab with Gözde Çetinkaya, who supported me through thick and thin. I would also like to thank Ozan Ertop for his sincere friendship, who is one of the most precious people I have met in two years. I would like to thank Akif Cem Heren for his joyful scientific conversations, all the collabrations we have made so far, and all the upcoming ones we will. Finally, I would like to thank Ömer Deniz Akyıldız for his kind friendship, his inspirations for my thesis, and most of it all, for his faith in me to be the researcher I dream of in the future.

The BUSIM family, I thank you all. I would like to thank Leda Sarı, who shared the same cubical with me for two years. I would also like to thank BETA family,

who are the most lively and joyful people on this earth. Especially, Gürkan Sönmez, who is my whiskey father now. I would also like to mention Engin Afacan, Gönenç Berkol, Berk Çamlı, Feyyaz Melih Akçakaya, Okan Zafer Batur, İsmail Kara, İskender Haydaroğlu, Hikmet Çeliker, and Melek Selcen Başar. You made my time more and more beautiful since I met you guys, I wish I had more time with you all.

ABSTRACT

ISI MITIGATION TECHNIQUES IN MOLECULAR COMMUNICATION

Molecular communication via diffusion (MCvD) is a new field of communication where molecules are used to transfer information. One of the main challenges in MCvD is the intersymbol interference (ISI), which inhibits communication at high data rates. Furthermore, at nano scale, energy efficiency becomes an essential problem. Before addressing these problems, a pre-determined threshold for the received signal must be calculated to make a decision. In this thesis, an analytical technique is proposed to determine the optimum threshold, whereas in the literature, these thresholds are usually calculated empirically. Since the main goal of this thesis is to build an MCvD system suitable for operating at high data rates without sacrificing quality, new modulation and filtering techniques are also proposed to decrease the effects of ISI and enhance energy efficiency. As the first transmitter-based solution, a modulation technique, molecular transition shift keying (MTSK), is proposed in order to increase the data rate by suppressing ISI. As the second transmitter-based solution, a pre-equalization method is proposed in which the transmitter utilizes two types of messenger molecules. Furthermore, for energy efficiency, a power adjustment technique that utilizes the residual molecules is proposed. Finally, as a receiver-based solution, a new energy efficient decision feedback filter (DFF) is proposed as a substitute for the conventional decoders in the literature. Error performance of all modulation techniques are presented in a comprehensive manner. Additionally, error performance of DFF and MMSE equalizers are compared in terms of bit error rates, and it is concluded that DFF may be more advantageous when energy efficiency is concerned, due to its lower computational complexity.

ÖZET

MOLEKÜLER İLETİŞİMDE SİMGELER ARASI GİRİŞİMİ AZALTMA TEKNİKLERİ

Difüzyon yoluyla moleküler iletişim, bilginin moleküller yoluyla iletimini konu alan yeni bir araştırma dalıdır. Moleküler iletişimde karşılaşılan en büyük problemlerden biri simgeler arası girişimdir, ve bu problem yüksek veri hızlarında iletişimi engellemektedir. Öte yandan, nano ölçekte harcanabilecek enerjinin kısıtlı olması da temel bir problemdir. Bu problemlere değinilmeden önce, verici tarafından algılanan molekül sayısını kullanarak sinyali geri oluşturabilmek için bir eşik değerinin belirlenmesi gerekmektedir. Bu tezde, literatürdeki empirik yöntemlerin aksine, en uygun eşik değerinin belirlenmesi için analitik bir teknik önerilmiştir. Bu tezin ana amacı yüksek veri hızlarında iletişim kalitesinden ödün vermeden çalışabilecek bir moleküler iletişim sistemi oluşturmak olduğundan, simgeler arası girişimi azaltmaya ve enerji tasarrufunu arttırmaya yönelik yeni modülasyon ve filtreleme tekniklerini önerilmiştir. Önerilen ilk verici bazlı çözüm, molekül tipi değişimiyle kodlama (MTDK) isimli yeni bir modülasyon tekniğidir. Önerilen ikinci verici bazlı çözüm ise, iki tip molekül kullanılarak uygulanan ön-denkleştirme tekniğidir. Enerji tasarrufunu arttırmak amacıyla da, kanalda arta kalan molekülleri kullanan bir enerji düzenleme tekniği önerilmiştir. Son olarak, verici bazlı bir çözüm olan geri beslemeli bir filtre önerilmiştir. Önerilen tüm modülasyon yöntemlerinin bit hata başarımları karşılaştırmalı bir biçimde sunulmuştur. Ek olarak, önerilen geri beslemeli filtrenin bit hata başarımı, en küçük ortalama hata denkleştiricisi ile karşılaştırılmış, ve geri beslemeli filtrenin enerji tasarrufu ve işlemsel karmaşıklık açısından daha üstün olduğu sonucuna varılmıştır.

TABLE OF CONTENTS

LIST OF FIGURES

LIST OF TABLES

LIST OF SYMBOLS

b_i	Message symbol in the ith time slot
$\hat{b}_i$	Estimate of b_i
$\mathbf{b}^n$	Binary message sequence of length n
C_i	Number of received molecules at the receiver in the ith time slot due to the transmission of $\mathbf{b}^n$
D	Diffusion coefficient
$\mathbf{d}_l^{\{i,j\}}$	A candidate sequence for $\mathbf{b}^i$
$f_{\text{hit}}(t)$	Hitting rate of molecules
$F_{\text{hit}}(t)$	Fraction of molecules absorbed by the receiver until time t
h_k	Coefficients of the FIR filter
$J_i(\gamma)$	Minimizing function considering all the candidate sequences.
K	Length of the FIR filter
M_{REC}	Number of received molecules at the receiver by sending M number of molecules for the first bit-1
M_i	Number of molecules sent from the transmitter in the ith time slot
$M_0(A)$	Number of type-A molecules emitted for bit-0
$M_1(A)$	Number of type-A molecules emitted for bit-1
$M_0(B)$	Number of type-B molecules emitted for bit-0
$M_1(B)$	Number of type-B molecules emitted for bit-1
p_k	Hitting probability for the k^{th} time slot.
$p(r, t \mid r_0)$	Molecule distribution function at time t and distance r given the initial distance r_0
$\bar{P}$	Average signal power
$P[b_i = 0]$	Probability of occurrence for bit-0 in the message sequence
$P[b_i = 1]$	Probability of occurrence for bit-1 in the message sequence
r	Distance of a molecule to the origin
r_0	Distance of the transmitter from the center of the receiver
r_r	Radius of the spherical receiver
S	Length of the receiver memory

t	Continious time variable
t_s	Symbol duration
α	Fraction of the average signal power dedicated to the primary signal
$\alpha_1, \alpha_0, \beta$	Linear regression parameters
$\gamma^{*\{i\}}$	Optimal threshold for the detection of b_i
Δx_i	Displacement of a molecule in the ith dimension
ζ	Stopping parameter of Algorithm 1
$\mu^{\{i\}}$	Expected number of molecules arriving at the receiver in the ith time slot
ρ	Step size of Algorithm 1
$\sigma^{2\{i\}}$	Variance of molecules arriving at the receiver in the ith time slot
τ	Time delay of the secondary signal
ω	Rate of reaction

LIST OF ACRONYMS/ABBREVIATIONS

BCSK	Binary concentration shift keying
BER	Bit error rate
BMoSK	Binary molecule shift keying
CSK	Concentration shift keying
DFE	Decision feedback equalizaer
DFF	Decision feedback filter
ISI	Inter symbol interference
MAP	Maximum a posteriori probability
MCSK	Molecule concentration shift keying
MCvD	Molecular communication via diffusion
ML	Maximum likelihood
MM	Messenger molecule
MMSE	Minimum mean square error
MoSK	Molecule shift keying
PA	Power adjustment
SIR	Signal to interference ratio

1. INTRODUCTION

Nanotechnology enables miniaturization and fabrication of devices in a scale ranging from 1 to 100 nanometers. At this scale, a nano-machine can be considered as the most basic functional unit [1]. Nano-machines are tiny components consisting of an arranged set of molecules, which are able to perform very simple computation, sensing, and/or actuation tasks [2]. They can be interconnected to form a nanonetwork, in which they can coordinate, share, and fuse information. At such small dimensions, electromagnetic communication is challenging because of physical implementation constraints, such as the ratio of the antenna size to the wavelength of the electromagnetic signal [1, 3]. Molecular communication is a new field of communication suitable for nanonetworks, where instead of electric currents or electromagnetic waves, patterns of molecules are used to transfer information from a source (transmitter) to a destination (receiver) [4]. In the literature, various molecular communication systems, such as molecular communication via diffusion (MCvD), calcium signaling, microtubules, pheromone signaling, and bacterium-based communication are proposed [5,6]. In this thesis, methods for improving the communication quality for an MCvD system are investigated.

A generic MCvD system includes five main processes: encoding, emission (transmission), propagation, absorption (reception), and decoding. Encoding is the process in which the transmitter encodes the information onto a physical property (e.g., number, type, etc.) of the messenger molecules. Emission is the process by which the transmitter releases the messenger molecules into the environment. In the propagation process, these molecules propagate through the environment following the physical characteristics of a channel. When some of these molecules arrive at the receiver (i.e., hit the receiver), they are sensed and absorbed by the receptors on the surface of the receiver, which is called the receiving process. Properties of these received molecules constitute the received signal and the received signal is decoded according to the encoding technique [4].

In the literature, several techniques are proposed for the encoding process. Concentration shift keying (CSK) and molecule shift keying (MoSK) are the most commonly used modulation techniques for nanonetworks [7–9] where communication is realized via diffusion. In CSK, number of received messenger molecules is used as the amplitude of the signal. In the case of binary CSK (BCSK), the receiver decodes the intended symbol as a bit-1 if the number of messenger molecules arriving at the receiver during a symbol duration exceeds a pre-determined threshold, and as a bit-0, otherwise. Binary MoSK (BMoSK), on the other hand, utilizes the emission of two different types of messenger molecules, where the transmitter releases the appropriate type of molecule based on the current symbol. The receiver then decodes the intended symbol based on the type and number of the molecules received during a time slot [10].

Problems that occur in an MCvD system can be grouped into two categories. The first category involves the problems caused by the random movements of the messenger molecules, i.e., diffusion. The random movement of the messenger molecules limits the amount of deterministic information about the received signal, therefore aggravates the decoding process. Notice that BCSK generally utilizes a *pre-determined* threshold at the receiver to make a decision for the received signal. In the literature, these threshold values are usually calculated empirically as follows: after the information transmission is over, the receiver calculates the bit error rate for various detection threshold values and chooses the optimal threshold that minimizes this error rate [10, 11]. This procedure requires the receiver to *know* the transmitted signal, which makes the communication process itself redundant. Another approach may be sending a long sequence of pilot symbols before the information transmission and calculate the optimal threshold empirically as described above. Problem with this approach arise due to the high sensitivity of the optimal threshold values both to the order and the value of the transmitted symbols. In order to have a sufficient representation of the system, one also has to send these pilot symbols repetitively, so that a comprehensive understanding of the system behavior can be obtained. Additionally, optimal threshold values are also sensitive to system parameters, i.e., if one of the system parameters, such as the diffusion coefficient, transmitter - receiver distance, etc. changes slightly,

this exhaustive procedure must be repeated. Although there is one attempt in the recent literature [12] to calculate the optimal threshold analytically, proposed calculations consider only the effect of one previous symbol, which is not sufficient for a diffusion channel at high data rates. As a result, more advanced problems of an MCvD system can not be properly addressed before solving the optimal thresholding problem. In this thesis, an analytical technique to determine the optimum threshold value prior to information transmission is proposed, which is the first main contribution of this thesis.

Another problem caused by diffusion is the inter symbol interference (ISI). Due to the nature of diffusion, some of the messenger molecules may fail to arrive at the receiver in their intended time slots and interfere with the messenger molecules of subsequent transmissions, causing ISI. One of the possible solutions to reduce the amount of ISI at the receiver is to keep the symbol duration as long as possible and, thus, allow the messenger molecules a longer time to reach their destinations. This effectively reduces the number of residual molecules left in the channel. On the other hand, increasing the symbol duration also decreases the data rate, which is already low compared to electromagnetic and optical channels due to the nature of diffusion.

The second category of problems arises due to the extremely small size of the nano scaled devices. Energy efficiency becomes a major constraint at nano scale [11] by limiting both the processing power of the communicating devices and their capacity to produce messenger molecules. Therefore, two different approaches can be considered for dealing with the energy efficiency problem in an MCvD system. First approach is to reduce the signal power, i.e., number of released molecules, as much as possible. The second approach is to reduce the power expended by a nano-machine during the encoding/decoding processes, which requires the design of filters or equalizers with minimal computational complexity. Both of these approaches would decrease the power consumption, while increasing the bit error rate. As a result, a trade off is observed between the data rate, energy efficiency, and communication quality.

The main goal of this thesis is to propose new techniques applicable at both transmitter and receiver sides, which can be chosen and implemented depending on the physical constraints of the nano machines. The proposed techniques aim to improve the overall communication quality to achieve arbitrarily low error rates at shorter symbol durations, hence increasing the data rate, while considering the energy constraints. Main contributions of this thesis can be summarized as follows.

- An analytical technique to determine the optimum threshold value prior to information transmission is proposed.
- A decision feedback filter for the decoding process, which has a lower computational complexity compared to a minimum mean squared error or decision feedback equalizer, is proposed.
- A new modulation technique, molecular transition shift keying (MTSK), is proposed, which is an energy efficient modulation technique designed to reduce the effects of ISI.
- A power adjustment technique that utilizes the residual molecules in the channel to enhance the energy efficiency, is proposed.
- A pre-equalization method is proposed in which the transmitter utilizes two types of messenger molecules.

Apart from the optimal threshold calculation, modulation and filtering techniques proposed in this thesis are potential solutions for MCvD systems under different constraints.

The remainder of this thesis is organized as follows: Chapter 2 reviews the characteristics of the diffusion process, modulation techniques in the literature, and the ISI problem. Receiver based ISI mitigation techniques that include the proposed analytical technique to determine the optimum threshold value for a nano communication system, proposed decision feedback filter (DFF) and the MMSE equalizer are given in Chapter 3. Chapter 4 introduces the transmitter based ISI mitigation techniques, which include the proposed modulation technique, MTSK, the power adjustment method ap-

plied to different modulation techniques, and the proposed pre-equalization technique. Chapter 5 concludes the thesis.

2. MOLECULAR COMMUNICATION VIA DIFFUSION AND ISI

2.1. System Model

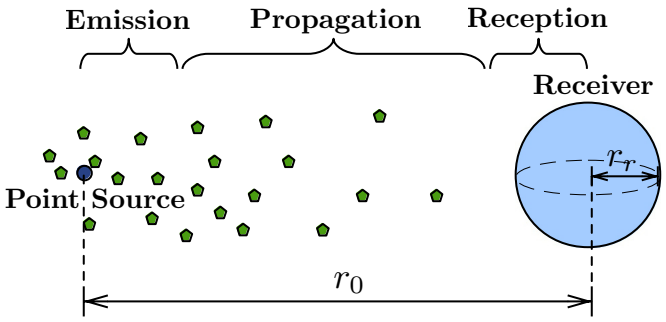

Figure 2.1. MCvD system model including a point source and a spherical receiver.

The communication model used in this thesis is depicted in Figure 2.1. Messenger molecules are used as information carriers between a point source and a spherical receiver with absorbing receptors. The point source is located at a distance r_0 from the center of the receiver. The point source and the spherical receiver both reside in a fluid propagation medium, which is an unbounded 3-dimensional (3-D) environment. After the information is modulated onto some physical property of the messenger molecules, these molecules are released to the medium, where they diffuse according to Brownian motion and arrive at the receiver. To receive the molecules (i.e. the signal), the spherical receiver with radius r_r uses receptors placed on its surface.

The messenger molecules are the information particles for an MCvD system. At this scale, random movement/diffusion of particles through the fluid is modeled by Brownian motion. The motion is governed by the combined forces applied to a messenger molecule by the molecules of the fluid due to thermal energy. Brownian motion is described by the Wiener process, which is a continuous-time stochastic process.

For simulating the Brownian motion in an n-dimensional space, time is divided

into 1 ms long steps for a variety of symbol durations in the order of 100 ms, and at each time step, random movement is applied to each dimension as

$$\vec{r}_{t+\Delta t} = \vec{r}_t + \Delta\vec{r}. \tag{2.1}$$

The total displacement of a molecule ($\Delta\vec{r}$) in one time step (Δt) can be found as

$$\Delta\vec{r} = (\Delta x_1, ..., \Delta x_n), \tag{2.2}$$

where Δx_i is the displacement of a molecule in the ith dimension. Movement in each dimension for a given time step is modeled independently and follows a Gaussian distribution, i.e., $\Delta x_i \sim \mathcal{N}(0, 2D\Delta t),\ \forall i \in \{1, ..., n\}$, where $\mathcal{N}(\mu, \sigma^2)$ denotes the Gaussian distribution with mean μ and variance σ^2. Molecules propagate in the environment according to these dynamics. As conventionally done in the literature, our model assumes that the molecules are dilute enough for the frequency of collisions to be insignificant, and therefore, ignores the collisions between the messenger molecules [13, 14]. Molecules within the receiver volume at the end of each time step is assumed to be absorbed. This model utilizing the Brownian motion is used for Monte Carlo simulations.

2.2. Absorption rate of a perfectly absorbing spherical receiver

The microscopic theory of diffusion can be developed from the assumption that a substance will move along its concentration gradient. The derivative of the flux with respect to time results in Fick's Second Law in a 3-D environment [15, Equation 3.60], given by

$$\frac{\partial p(r, t|r_0)}{\partial t} = D\nabla^2 p(r, t|r_0), \tag{2.3}$$

where ∇^2, $p(r, t|r_0)$, and D are the Laplacian operator, the molecule distribution function at time t and distance r (distance of molecules from their initial position)

given the initial distance r_0, and the diffusion constant, respectively. The value of D depends on the temperature, the viscosity of the fluid, and the Stokes' radius of the molecule [16].

Fraction of molecules hitting a perfectly absorbing spherical receiver located at $(0, 0, 0)$ has been recently derived in [15] by solving the Fick's diffusion equation with relevant initial and boundary conditions and describing the absorbing process. The initial condition is defined as [15, Equation 3.61]

$$p(r, t \to 0|r_0) = \frac{1}{4\pi r_0^2}\delta(r - r_0). \tag{2.4}$$

The first boundary condition is [15, Equation 3.63]

$$\lim_{r\to\infty} p(r, t|r_0) = 0, \tag{2.5}$$

which reflects the assumption that the distribution of the molecules vanishes at distances far greater than r_0. The second boundary condition is [15, Equation 3.64]

$$D\frac{\partial p(r, t|r_0)}{\partial r} = wp(r, t|r_0) \text{ for } r = r_r, \tag{2.6}$$

where r_r and w denote the radius of the receiver and the rate of reaction, respectively. When the rate of reaction approaches infinity, it corresponds to the boundary condition in which every collision leads to an absorption. In other words, receiver is completely covered with receptors and all receptors are perfectly absorbing. In this case, we consequently have a diminishing $p(r, t|r_0)$ as r approaches the surface of the absorber (i.e., $\lim_{r\to r_r} p(r, t|r_0) = 0$).

After solving the differential equation for $w \to \infty$ for the perfectly absorbing sphere with the given boundary and initial conditions, the molecule distribution func-

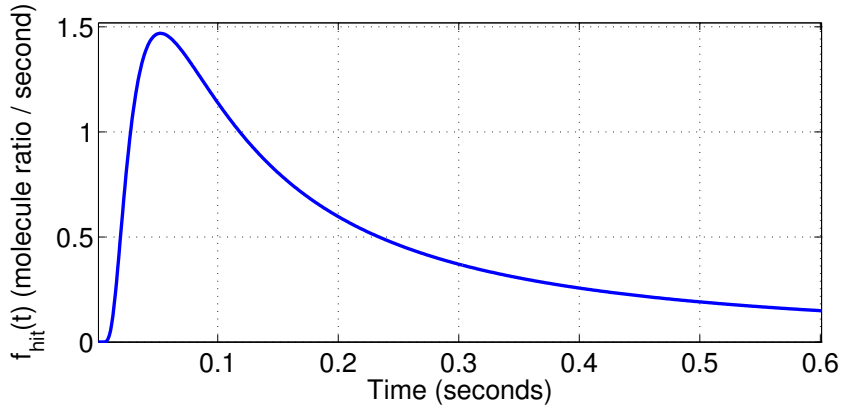

Figure 2.2. $f_{\text{hit}}(t)$ for $r_r = 5\mu m$, $r_0 = 10\mu m$, and $D = 79.4\mu m^2/s$.

tion at time t and distance r is obtained as [15, Equation. 3.104]

$$p(r,t|r_0) = \frac{1}{4\pi r r_0}\frac{1}{\sqrt{4\pi Dt}} \times \left(e^{-\frac{(r-r_0)^2}{4Dt}} - e^{-\frac{(r+r_0-2r_r)^2}{4Dt}} \right). \tag{2.7}$$

Using (2.7), the hitting rate of molecules is also calculated in [15, Equation 3.108] as

$$f_{\text{hit}}(t) = 4\pi r_r^2 \; w \; p(r_r,t|r_0) = \frac{r_r}{r_0}\frac{1}{\sqrt{4\pi Dt}}\frac{r_0 - r_r}{t} \; e^{-\frac{(r_0-r_r)^2}{4Dt}}, \tag{2.8}$$

which is illustrated in Figure 2.2 for $r_r = 5\mu m$, $r_0 = 10\mu m$, and $D = 79.4\mu m^2/s$ [1] . Note that $[f_{\text{hit}}(t)]$ = molecule ratio / second, which corresponds to the fraction of released molecules that hits the receiver per unit time.

Furthermore, integrating $f_{\text{hit}}(t)$, fraction of molecules absorbed by the receiver until time t, $F_{\text{hit}}(t)$, can be obtained as [15, Equation 3.116]

$$F_{\text{hit}}(t) = \int_0^t f_{\text{hit}}(t')dt' = \frac{r_r}{r_0} \; \text{erfc} \left[\frac{r_0 - r_r}{\sqrt{4Dt}} \right]. \tag{2.9}$$

[1] These values are considered to be typical, since they simulate an environment where human insulin hormone is used as the messenger molecules, and a device whose capabilities are similar to a pancreatic β-cell is used as the tranmistter [11].

Time dependent formulation for the fraction of molecules absorbed by the receiver is an important formulation in the nanonetworking domain, since (2.8) and (2.9) describe the response of the diffusion channel completely.

2.3. Modulation and demodulation techniques

BCSK and BMoSK are the two most common modulation techniques for MCvD. In BCSK, number of the received messenger molecules is used as the amplitude of the signal. The receiver decodes the intended symbol as a bit-1 if the number of messenger molecules arriving at the receiver during a time slot exceeds a pre-determined threshold, and as a bit-0, otherwise. To represent different values of symbols, the transmitter releases different number of molecules for each value the symbol can represent, e.g., the transmitter releases n_0 molecules for a bit-0, whereas it releases n_1 molecules for a bit-1 [10]. As mentioned earlier, in the literature, the threshold is typically empirically chosen by using a long sequence of pilot symbols.

The BMoSK, on the other hand, utilizes the emission of two different types of messenger molecules to represent information. The transmitter releases a constant number of type-A or type-B molecules for the current symbol values of bit-0 and bit-1, respectively. The receiver then decodes the intended symbol side on the type and the number of the molecules received during a time slot [10]. Unlike BCSK, decoding of a BMoSK encoded binary sequence does not necessarily require a threshold value. The receiver can make a decision simply by comparing the received number of molecules of both molecule types and determining which one is larger.

The MCvD system using BCSK can be adversely affected from ISI, caused by the residual molecules from the previous symbols [10]. By using (2.8), the hitting rates for a BCSK encoded binary message sequence of $\{1, 1, 0, 1, 0, 1, 1\}$ are calculated, and effects of ISI on each time slot are illustrated in Figure 2.3a.

Similar to the BCSK, the residual molecules from the previous symbols also cause ISI when BMoSK is used. BMoSK is less susceptible to ISI effects than the BCSK

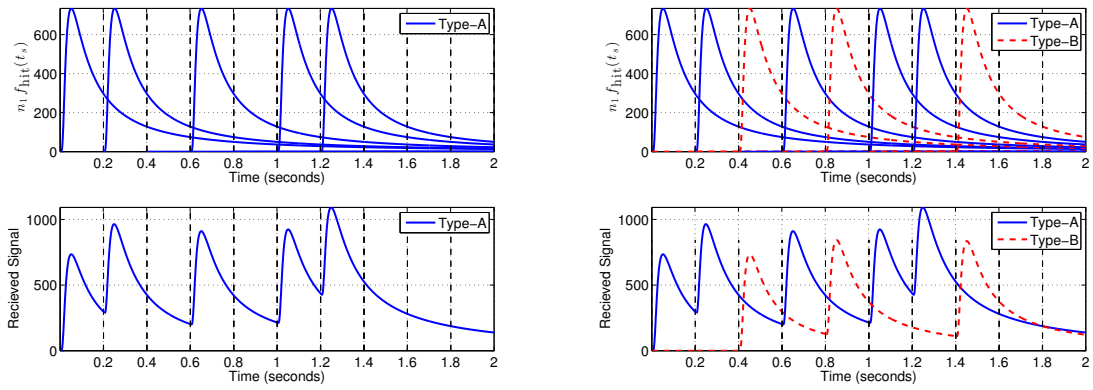

a b

Figure 2.3. Effects of ISI where $r_r = 5\mu m$, $r_0 = 10\mu m$, $D = 79.4\mu m^2/s$, $n_0 = 0$, $n_1 = 500$ and $t_s = 200ms$ for (a) BCSK encoded sequence and (b) BMoSK encoded sequence of $\{1, 1, 0, 1, 0, 1, 1\}$.

technique [10]. However, BMoSK requires the synthesis of two types of molecules rather than one, and number of molecules released from transmitter almost doubles, since bit-0s are also encoded with constant number of molecules. Effects of ISI for BMoSK is illustrated in Figure 2.3b, where the same binary message sequence of $\{1, 1, 0, 1, 0, 1, 1\}$ is used.

In conclusion, both modulation techniques are inefficient in terms of energy efficiency and ISI mitigation when molecular communication at high data rates is considered. Additionally, there is no technique in the literature besides the empirical one to calculate the threshold value for a BCSK encoded sequence.

3. RECEIVER BASED ISI MITIGATION TECHNIQUES

3.1. ISI threshold computation technique

In the literature, the optimal threshold is usually assumed to be calculated after the information transmission is over, which requires the receiver to *know* the transmitted signal, and makes the communication process itself redundant. The error rates obtained after such thresholding would provide a lower bound for the bit error rates, rather than a realistic result. There are also different approaches in the literature on the design of an optimal receiver for a BCSK [17, 18], or BMoSK encoded sequence [19], which are elegant solutions but too complex in terms of computation for a nanomachine implementation. As an alternative, another approach may be transmitting a sufficiently long sequence of pilot symbols before the information transmission in order to obtain a comprehensive model of the system behavior. The problem with this approach arises due to the high sensitivity of the optimal threshold values both to the order and the value of the transmitted symbols. Therefore, one also has to retransmit these pilot symbols frequently to obtain a reliable model of the channel behavior. Additionally, the optimal threshold values are also sensitive to system parameters, meaning that if one of the system parameters, such as diffusion coefficient, transmitter - receiver distance, etc., changes slightly, this exhaustive procedure must be repeated. This is the main motivation for developing an analytical approach to calculate the optimal threshold.

By using $F_{\text{hit}}(t)$ given in (2.9), probability of a single molecule to hit the receiver in a given time slot can be calculated. Let p_k denote the hitting probabilities, where p_1 is the hitting probability in the current symbol duration and p_k for $k \geq 2$ denote the hitting probabilities in the consecutive symbol durations. Hitting probabilities p_k for $k = 1, 2, ...$ for a given system model can be calculated using

$$p_k = F_{\text{hit}}(kt_s) - F_{\text{hit}}([k-1]ts) \tag{3.1}$$

where t_s denotes the symbol duration.

Hitting probabilities are sufficient to describe the characteristics of the diffusion channel completely, which implies that the choice of symbol duration has a great significance in determination of the channel response. In terms of ISI mitigation, it is desirable to have p_1 to be the largest in magnitude compared to p_k for $k > 1$. Therefore, t_s should be chosen such that hitting probabilities are in descending order ($p_1 > p_2 > p_3 > ...$).

Let $\mathbf{b}^n = \{b_1, b_2, ..., b_n\}$ denote the binary message sequence of length n, and let b_i and M_i denote the message symbols and number of molecules sent from the transmitter in the ith time slot for $i = 1, 2, ..., n$, respectively. For simplicity, assume BCSK, where the number of molecules to be transmitted is $M_i = M$ for $b_i = 1$, and $M_i = 0$ for $b_i = 0$.

When the number of transmitted molecules is high, the number of received molecules at the receiver for a given time slot can be approximated by a Poisson or a Gaussian random variable (depending on the system parameters) [4, 20]. Considering the parameters used throughout this thesis, it is concluded that Gaussian model describes the arrival process with a better accuracy compared to Poisson model [20]. As a result, Gaussian approximation is chosen to model the number of received molecules.

Let C_i denote the number of received molecules at the receiver in the ith time slot due to the transmission of $\mathbf{b}^i$. The probability model for C_i can be defined [4] as

$$b_i \sim \mathcal{BE}(P[b_i = 1]), \tag{3.2}$$

$$C_i|\mathbf{b}^i \sim \mathcal{N}(\mu^{\{i\}}, \sigma^{2\{i\}}), \tag{3.3}$$

where $\mathcal{BE}(\cdot)$, $\mathcal{N}(\cdot, \cdot)$, $P[b_i = 1]$, and $P[b_i = 0]$ denote the Bernoulli distribution, Gaussian distribution, probability of occurrence for bit-1 and probability of occurrence for bit-0 in the message sequence, respectively.

Due to ISI, the expected number of molecules arriving at the receiver in the ith time slot can be given as

$$\mathrm{E}[C_i|\mathbf{b}^i] = \mu^{\{i\}} = M \sum_{k=1}^{i} p_k \, b_{i-k+1}, \tag{3.4}$$

which is the mean of the Gaussian distributed molecule count at the receiver. The variance of C_i is similarly given by

$$\mathrm{Var}[C_i|\mathbf{b}^i] = \sigma^{2\{i\}} = M \sum_{k=1}^{i} p_k \left(1 - p_k\right) b_{i-k+1}. \tag{3.5}$$

It should be noted that (3.4) and (3.5) do not include any randomness except for the one due to the diffusion process. This model can be extended by the addition of a zero-mean white Gaussian noise with a constant variance σ_c^2, which may represent the counting noise at the receiver, or noise due to the molecule reactions in the environment, etc. Since the sum of two independent Gaussian random variables is again a Gaussian random variable, with its mean being the sum of the two means, and its variance being the sum of the two variances, the variance of C_i becomes

$$\sigma^{2\{i\}} = \sigma_c^2 + M \sum_{k=1}^{i} p_k \left(1 - p_k\right) b_{i-k+1}. \tag{3.6}$$

Equations 3.4 and 3.5 indicate that the parameters of the Gaussian distribution change for each symbol, which means that each and every symbol requires its own optimal threshold. To begin with, let us focus on finding the optimal threshold $\gamma^{*\{i\}}$

for the detection of b_i in $\mathbf{b}^n$ such that

$$C_i \underset{\hat{b}_i=0}{\overset{\hat{b}_i=1}{\gtrless}} \gamma^{*\{i\}}, \tag{3.7}$$

where $\hat{b}_i$ denotes the estimate of b_i. Note that in the case of $C_i = \gamma^{*\{i\}}$, the receiver can be preset to decide for a bit-0 or bit-1, or choose one of them randomly. We can treat this case as a traditional binary detection problem in an AWGN channel and use *maximum a posteriori probability* (MAP) decision rule, given as

$$\frac{P[b_i = 1]\, p(C_i \mid \mathbf{b}^{i-1}, b_i = 1)}{P[b_i = 0]\, p(C_i \mid \mathbf{b}^{i-1}, b_i = 0)} \underset{\hat{b}_i=0}{\overset{\hat{b}_i=1}{\gtrless}} 1, \tag{3.8}$$

where $p(\cdot)$ denotes the probability density function of the Gaussian distributed C_i. Note that calculation of $\gamma^{*\{i\}}$ requires information about the sequence history $\mathbf{b}^{i-1}$. In case of a memoryless decoder, when the first $(i-1)$ bits, which are crucial for (3.4) and (3.5), are unknown, all possible combinations (candidates) for $\mathbf{b}^{i-1}$ must be considered, which yields 2^{i-1} candidate means, variances, and optimal thresholds. Each $\mathbf{b}^{i-1}$ candidate also has its own probability, $P[\mathbf{b}^{i-1}]$. Let $\mathbf{d}_l^{\{i,j\}} = \{d_l^{\{i,j\}}[1], d_l^{\{i,j\}}[2], ..., d_l^{\{i,j\}}[i]\}$ denote a candidate sequence for $\mathbf{b}^i$, i.e., a possible binary sequence combination of length i, and $\gamma^{*\{i,j\}}$ denote its corresponding optimal threshold value. In this notation, l denotes whether the candidate sequence is conditioned on $b_i = 0$ or $b_i = 1$, and j is equal to the decimal value of reverse ordered $\mathbf{d}_l^{\{(i-1),j\}}$ sequence, such that

$$j = \sum_{z=1}^{i-1} d_l^{\{i,j\}}[z] 2^{z-1}, \tag{3.9}$$

where $\mathbf{d}_l^{\{(i-1),j\}}$ denotes the first $(i-1)$ bits of $\mathbf{d}_l^{\{i,j\}}$. For example, for a bit sequence of length $n = 3$, there are $2^3 = 8$ possible candidate sequences, which are visualized as a binary tree given in Figure 3.1. One of the candidates is $\mathbf{d}_0^{\{3,1\}}$, which corresponds to

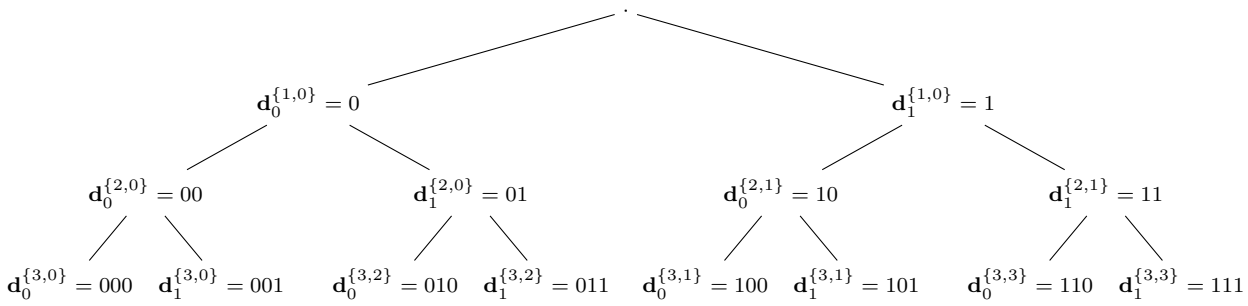

Figure 3.1. Binary tree for $n = 3$.

the bit sequence of length three, conditioned on bit-0, and with decimal value 1 for the reverse ordered history; which can only be the sequence $\{1\,0\,0\}$. Calculating j allows for the enumeration of candidates with respect to the amount of ISI they induce, since the latter symbols contribute more to the ISI than the former ones.

By conditioning each candidate on bit-1 and bit-0, the optimal threshold $\gamma^{*\{i,j\}}$ can be found for siblings $\{\mathbf{d}_0^{\{i,j\}}, \mathbf{d}_1^{\{i,j\}}\}$ in the binary tree, which are basically two Gaussian distributions with parameter sets $\{\mu_0^{\{i,j\}}, \sigma_0^{\{i,j\}}\}$ and $\{\mu_1^{\{i,j\}}, \sigma_1^{\{i,j\}}\}$, respectively. Each $\gamma^{\{i,j\}}$ can be calculated by writing (3.8) and (3.7) explicitly, which yields

$$P[b_i = 1]p(\gamma^{*\{i\}} \mid \mathbf{b}^{i-1}, b_i = 1) = P[b_i = 0]p(\gamma^{*\{i\}} \mid \mathbf{b}^{i-1}, b_i = 0), \tag{3.10}$$

$$\log\left[\frac{\sqrt{2\pi\sigma_0^{2\{i,j\}}}}{\sqrt{2\pi\sigma_1^{2\{i,j\}}}}\frac{\exp\big(-(\gamma^{*\{i\}} - \mu_1^{\{i,j\}})^2/2\sigma_1^{2\{i,j\}}\big)}{\exp\big(-(\gamma^{*\{i\}} - \mu_0^{\{i,j\}})^2/2\sigma_0^{2\{i,j\}}\big)}\right] = \log\Big[\frac{P[b_i = 0]}{P[b_i = 1]}\Big], \tag{3.11}$$

resulting in the quadratic equation

$$a\left(\gamma^{*\{i\}}\right)^2 + b\gamma^{*\{i\}} + c = 0, \tag{3.12}$$

where,

$$a = \left[\sigma_1^{2\{i,j\}} - \sigma_0^{2\{i,j\}}\right], \tag{3.13}$$

$$b = 2\left[\sigma_0^{2\{i,j\}}\mu_1^{\{i,j\}} - \sigma_1^{2\{i,j\}}\mu_0^{\{i,j\}}\right], \tag{3.14}$$

$$c = \sigma_1^{2\{i,j\}}\mu_0^{2\{i,j\}} - \sigma_0^{2\{i,j\}}\mu_1^{2\{i,j\}} - 2\sigma_1^{2\{i,j\}}\sigma_0^{2\{i,j\}}\log\left[\frac{P[b_i=0]\sigma_1^{\{i,j\}}}{P[b_i=1]\sigma_0^{\{i,j\}}}\right]. \tag{3.15}$$

This equation can be solved analytically considering the positive root $\gamma^{*\{i\}} = \frac{-b+\sqrt{\Delta}}{2a}$, where $\Delta = b^2 - 4ac$.

To find the optimal threshold $\gamma^{*\{i\}}$ that minimizes the overall probability of error in the detection of b_i considering all candidate sequences, the minimizing function can be written as

$$J_i(\gamma) = \sum_{j=0}^{2^{i-1}-1} P[\mathbf{d}_0^{\{i,j\}}]Q\left(\frac{\gamma - \mu_0^{\{i,j\}}}{\sigma_0^{\{i,j\}}}\right) + P[\mathbf{d}_1^{\{i,j\}}]Q\left(\frac{\mu_1^{\{i,j\}} - \gamma}{\sigma_1^{\{i,j\}}}\right),\ \forall i \geq 1, \tag{3.16}$$

which is equal to the sum of error probabilities for a given threshold γ. To minimize $J_i(\gamma)$, derivative with respect to γ can be set to zero as

$$\frac{\partial J_i(\gamma)}{\partial \gamma} = \sum_{j=0}^{2^{i-1}-1} P[\mathbf{d}_1^{\{i,j\}}]\mathcal{N}(\gamma^{*\{i\}}|\mu_1^{\{i,j\}}, \sigma_1^{2\{i,j\}}) - P[\mathbf{d}_0^{\{i,j\}}]\mathcal{N}(\gamma^{*\{i\}}|\mu_0^{\{i,j\}}, \sigma_0^{2\{i,j\}}) = 0, \tag{3.17}$$

which yields

$$\sum_{j=0}^{2^{i-1}-1} P[\mathbf{d}_1^{\{i,j\}}]\mathcal{N}(\gamma^{*\{i\}}|\mu_1^{\{i,j\}}, \sigma_1^{2\{i,j\}}) = \sum_{i=1}^{2^{i-1}-1} P[\mathbf{d}_0^{\{i,j\}}]\mathcal{N}(\gamma^{*\{i\}}|\mu_0^{\{i,j\}}, \sigma_0^{2\{i,j\}}). \tag{3.18}$$

For $i > 2$, (3.18) becomes a hard problem to solve analytically due to the combinatorial nature of the equation, so numerical methods are used instead.

$\gamma^{*\{i\}}$ can be efficiently computed using two fundamental observations. The first

observation makes use of (3.4), (3.5), and the fact that t_s is chosen such that hitting probabilities are in an descending order, i.e., $p_i > p_j$ for $i < j$. We can then sort the distribution parameters as

$$\begin{aligned}
&\mu_0^{\{i,1\}} < \mu_0^{\{i,2\}} < ... < \mu_0^{\{i,2^{i-1}-1\}},\\
&\mu_1^{\{i,1\}} < \mu_1^{\{i,2\}} < ... < \mu_1^{\{i,2^{i-1}-1\}},\\
&\sigma_0^{\{i,1\}} < \sigma_0^{\{i,2\}} < ... < \sigma_0^{\{i,2^{i-1}-1\}},\\
&\sigma_1^{\{i,1\}} < \sigma_1^{\{i,2\}} < ... < \sigma_1^{\{i,2^{i-1}-1\}}.
\end{aligned} \tag{3.19}$$

Consequently, optimal thresholds can also be sorted as

$$\gamma^{*\{i,1\}} < \gamma^{*\{i,2\}} < ... < \gamma^{*\{i,2^{i-1}-1\}}. \tag{3.20}$$

Being able to sort these optimal thresholds provides us with an upper bound $\gamma^{*\{i,2^{i-1}-1\}}$, since the optimal threshold considering all candidates cannot be greater than the optimal threshold considering only the siblings $\{\mathbf{d}_0^{\{i,2^{i-1}-1\}}, \mathbf{d}_1^{\{i,2^{i-1}-1\}}\}$ with the highest mean and variance values, i.e., $\gamma^{*\{i\}} < \gamma^{*\{i,2^{i-1}-1\}}$.

The second observation is that, as n increases, due to the accumulating molecules in the diffusion channel, the optimal threshold also increases monotonically, i.e., $\gamma^{*\{i-1\}} < \gamma^{*\{i\}}$. In conclusion, the lower and upper bounds for $\gamma^{*\{i\}}$ can be written as

$$\gamma^{*\{i-1\}} < \gamma^{*\{i\}} < \gamma^{*\{2^{i-1}-1\}}. \tag{3.21}$$

These bounds allow for the search of $\gamma^{*\{i\}}$ by employing a fixed point iteration. Such an iterative algorithm is given in Algorithm 1, where ρ and ζ denote the step size and stopping parameter of the algorithm, respectively. The first 25 threshold values computed using Algorithm 1 are shown in Figure 3.2. The step size ρ is initialized to $M/100$, since the threshold value will be proportional to the number of molecules transmitted for $b_i = 1$. Additionally, a proper choice for ζ would be 1, since the algo-

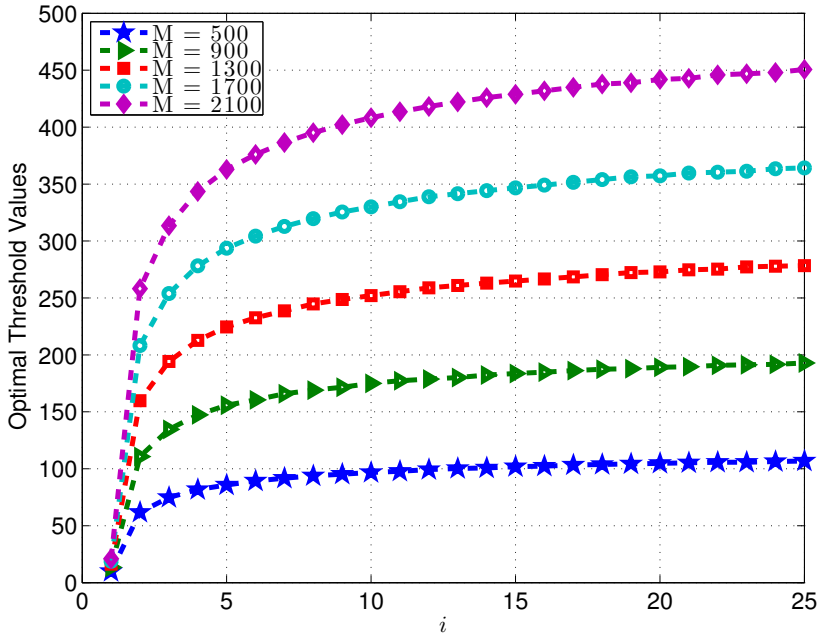

Figure 3.2. Optimal threshold values for $i \leq 25$, where $P[b_i = 0] = 0.5$ and $t_s = 200ms$.

rithm is searching a value which has the unit of molecules. Although the calculations are conducted using $\zeta = 10^{-4}$ in the manuscript, on a practical level, having an integer threshold value would be more meaningful, since the number of received molecules will be an integer as well.

Example 3.1. *Consider a BCSK modulated random binary sequence, where* $P[b_i = 0] = P[b_i = 1] = 0.5$, $\forall i$. *To calculate the optimal threshold* $\gamma^{*\{2\}}$, *the distribution parameters must be calculated by using (3.4) and (3.5). Candidate sequences and their corresponding parameters are given in Table 3.1.*

To calculate $\gamma^{*\{2\}}$, *(3.4) and (3.5) must be used, which means that information of the first two hitting probabilities are required. Let us define a parameter set, denoted by* $\mathcal{P}$, *where* $r_r = 5\mu m$, $r_0 = 10\mu m$, $\sigma_c^2 = 1$, *molecules similar to insulin hormone are used as information carriers, and the channel is filled with a liquid which results in a diffusion coefficient of* $79.4\mu m^2/s$ *[11]. This parameter set will be used for all the latter simulations and examples in this thesis. For this example, in addition to*

the set of parameters $\mathcal{P}$, the symbol duration is chosen as $t_s = 200ms$, and $M = 100$ molecules are used as messenger molecules on each symbol duration.

According to (3.10), $\gamma^{*\{2,0\}}$ is the intersection point of the two Gaussian distributions that arise due to $\mathbf{d}_0^{\{2,0\}}$ and $\mathbf{d}_1^{\{2,0\}}$, where the likelihoods are equal to each other. Likewise, $\gamma^{*\{2,1\}}$ is the intersection point of the two Gaussian distributions that arise due to $\mathbf{d}_0^{\{2,1\}}$ and $\mathbf{d}_1^{\{2,1\}}$. Thus, $\gamma^{*\{2,0\}}$ and $\gamma^{*\{2,1\}}$ must satisfy

$$0.5\mathcal{N}(\gamma^{*\{2,0\}}|\mu_0^{\{2,0\}}, \sigma_0^{2\{2,0\}}) = 0.5\mathcal{N}(\gamma^{*\{2,0\}}|\mu_1^{\{2,0\}}, \sigma_1^{2\{2,0\}}), \tag{3.22}$$

$$0.5\mathcal{N}(\gamma^{*\{2,1\}}|\mu_0^{\{2,1\}}, \sigma_0^{2\{2,1\}}) = 0.5\mathcal{N}(\gamma^{*\{2,1\}}|\mu_1^{\{2,1\}}, \sigma_1^{2\{2,1\}}). \tag{3.23}$$

On the other hand, $\gamma^{*\{2\}}$ must satisfy (3.18), and requires equating the sum of likelihoods for $\mathbf{d}_0^{\{2,j\}}$ and $\mathbf{d}_1^{\{2,j\}}$ for $j = \{0, 1\}$, which yields

$$\begin{aligned} 0.25\mathcal{N}(\gamma^{*\{2\}}|\mu_0^{\{2,0\}}, \sigma_0^{2\{2,0\}}) + 0.25\mathcal{N}(\gamma^{*\{2\}}|\mu_0^{\{2,1\}}, \sigma_0^{2\{2,1\}}) = \\ 0.25\mathcal{N}(\gamma^{*\{2\}}|\mu_1^{\{2,0\}}, \sigma_1^{2\{2,0\}}) + 0.25\mathcal{N}(\gamma^{*\{2\}}|\mu_1^{\{2,1\}}, \sigma_1^{2\{2,1\}}). \end{aligned} \tag{3.24}$$

Equations (3.22) and (3.23) can be solved analytically, and more importantly, as i increases, calculating $\gamma^{*\{i,j\}}$ for $j = \{0, 1, ..., 2^{i-1} - 1\}$ requires solving 2^{i-1} separate equations, which are individually analytically solvable. On the other hand, $\gamma^{*\{2\}}$ in (3.24) is hard to solve for analytically, and becomes harder due to the combinatorial nature of (3.18) as i increases, hence requires the use of Algorithm 1.

Distribution of candidate sequences and threshold values for this example are plotted in Figure 3.3. These results can be interpreted as follows. If the receiver is memoryless, it has to consider all possible candidate sequences in order to make a decision for b_2. In this case, $\gamma^{*\{2\}}$ must be used, meaning that any number of molecules below approximately 13 molecules yields a decision of $\hat{b}_2 = 0$. On the other hand, if

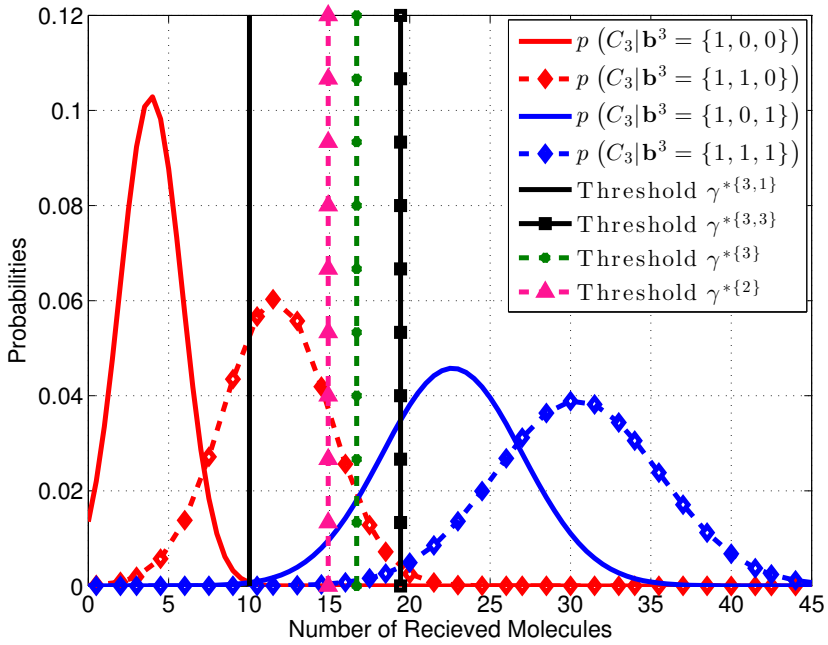

Figure 3.3. Distributions of received molecule counts and threshold values.

the receiver stores information about $\hat{b}_1$, depending on the binary value of $\hat{b}_1$, either $\gamma^{*\{2,0\}}$ or $\gamma^{*\{2,1\}}$ can be used.

3.1.1. Linear Regression

Computing the optimal threshold for b_i requires computation of the distribution parameters for all candidates, which means that the number of operations increases with powers of 2 as i increases. However, in the case of a continuous transmission, the optimal threshold must be calculated for very long sequences of bits, i.e., as $i \to \infty$. In order to predict $\gamma^{*\{i\}}$ for large values of i, common transforms are applied to i values, in the form of [21, Equation 10.8]

$$\gamma^{*\{i\}} = \alpha_1 i^{-\beta} + \alpha_0, \tag{3.25}$$

where $\alpha_0, \alpha_1 \in \mathbb{R}$, and $0 < \beta < 1$. This transformation enables to use linear regression techniques more effectively with nonlinear data given in Figure 3.2. As seen in Figure 3.4, there is a linear relationship between $1/\sqrt{i}$ and the optimal threshold values $\gamma^{*\{i\}}$

for $i \geq 3$ ($i = 3$ is denoted with a dashed vertical line), where $t_s = 200\,\text{ms}$ and $M = 500$. As a result, linear regression can be applied to calculate the the threshold values $\gamma^{*\{i\}}$ for $3 \leq i \leq 25$, using (3.25) where $\beta = 0.5$.

The motivation of using a function of this from can be justified based on two facts. First, note that hitting probabilities have a cumulative effect on both distribution parameters, as seen in (3.4) and (3.5). As i increases, the marginal effect of hitting probabilities will decrease, indicating that there should be a limit value as i goes to infinity. Physical interpretation of this is as follows: since the channel is assumed to be free of molecules before the transmission begins, the optimal threshold value will increase in the early stages of the transmission. As transmission continues, due to the accumulation of the molecules in the diffusion channel, number of molecules in the channel will go into saturation and the optimal threshold value will converge to a constant.

To verify the reliability of the linear regression outputs, 1000 random binary messages, consisting of 100 equally likely bits, are generated, and the empirical thresholds for each i are calculated such that the error rate for each b_i is minimized by considering all the 1000 realizations at the same time. This is repeated for 500 times, and the results are presented in Figure 3.5. As can be seen from the figure, linear regression outputs follow the mean of the empirically chosen thresholds, which verifies the performance of the linear regression and Algorithm 1.

It should be noted that β, α_0, and α_1 in (3.25) are dependent on both M and hitting probabilities p_k, since the mean and variance of the molecule counts at the receiver are also dependent on them, as given in (3.4) and (3.6). Furthermore, hitting probabilities are determined by both the symbol duration t_s and the environmental parameters such as diffusion coefficient, receiver radius, etc. As a result, if one of these parameters change, β, α_0, and α_1 must be calculated accordingly.

Since it is possible to compute $\gamma^{*\{i\}}$, $\forall i$, and $\lim_{i\to\text{inf}} \gamma^{*\{i\}} = \alpha_0$, different strategies can be used for thresholding. A realistic scenario could be as follows: receiver

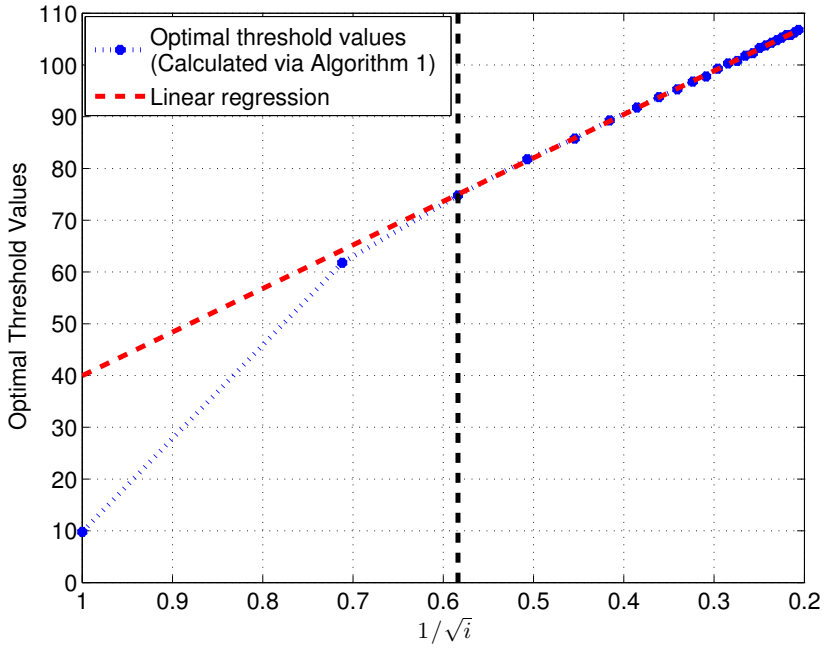

Figure 3.4. Linear relationship between $1/\sqrt{i}$ and $\gamma^{*\{i\}}$ for $i \leq 25$, where $P[b_i = 0] = 0.5$, $t_s = 200\,\text{ms}$.

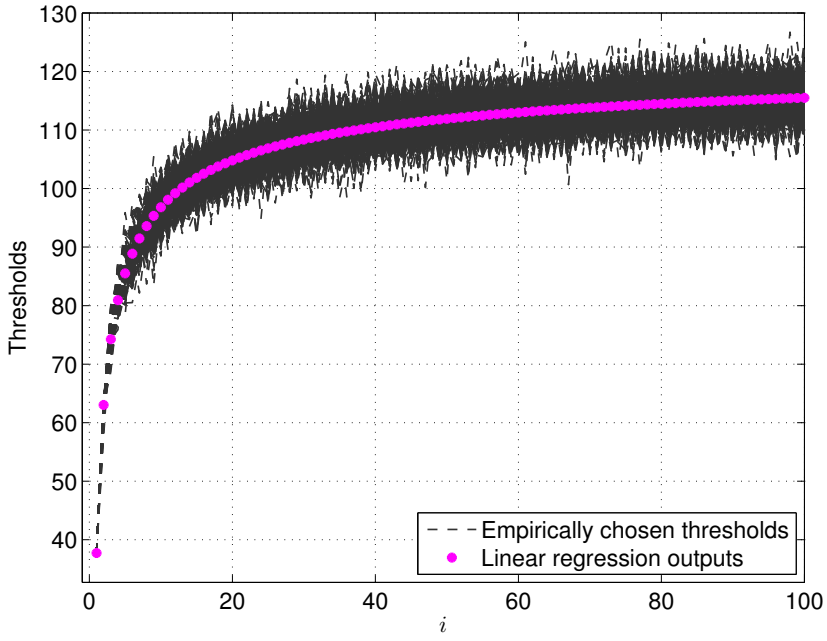

Figure 3.5. Comparison of empirical threshold values and linear regression outputs, where $P[b_i = 0] = 0.5$, $t_s = 200\,\text{ms}$, and $M = 500$.

senses the environmental parameters and calculates the hitting probabilities using (3.1). Using these parameters and Algorithm 1, it can calculate the first n optimal thresholds and then apply the linear regression given in (3.25) for a range of values for β to arrive at the optimal set of $\{\beta, \alpha_0, \alpha_1\}$, which minimizes the root mean squared error (RMSE) between the data points and the linear regression outputs. Note that the accuracy will depend on the number of thresholds calculated in the first step. After obtaining the values for β, α_0, and α_1, the receiver can then implement one of the following strategies:

- Strategy 1 : Since optimal threshold values converge to a constant ($\lim_{i\to\infty} \gamma^{*\{i\}} = \alpha_0$), the receiver decodes each b_i independent of i using α_0 as the threshold.
- Strategy 2 : Receiver decodes each b_i depending on i, i.e., it calculates $\gamma^{*\{i\}}$ for each i, using α_1 and α_0.

Note that, in case of a change in system parameters, the receiver can re-calculate β, α_0, and α_1, which is much more efficient than utilizing a long sequence of pilot symbols each time there is a slight change in the environment.

A performance comparison between the proposed strategies and the empirically computed thresholds is given in Figure 3.6. Binary sequences of length 10^5 were used in the simulations and 100 iterations were realized to take an average. RMSE of the linear regression outputs are calculated for each M and t_s to find the optimal β values. Empirical thresholds were calculated by trying various number of threshold values and minimizing the Hamming distance $d_H(\hat{\mathbf{b}}^n, \mathbf{b}^n)$ after gathering all the information about molecule counts at the receiver, which means that they provide a lower bound to the bit error rate. Thresholding strategy 2 performs slightly better compared to strategy 1, as expected, since it adjusts the threshold value for every i. As the symbol duration increases, the lower bound for bit error rate decreases, hence the gap between the proposed strategies and the lower bound increases. As a result, both strategies provide a solution for the thresholding problem with noteworthy error rate results, which was not addressed in a comprehensive manner in the literature.

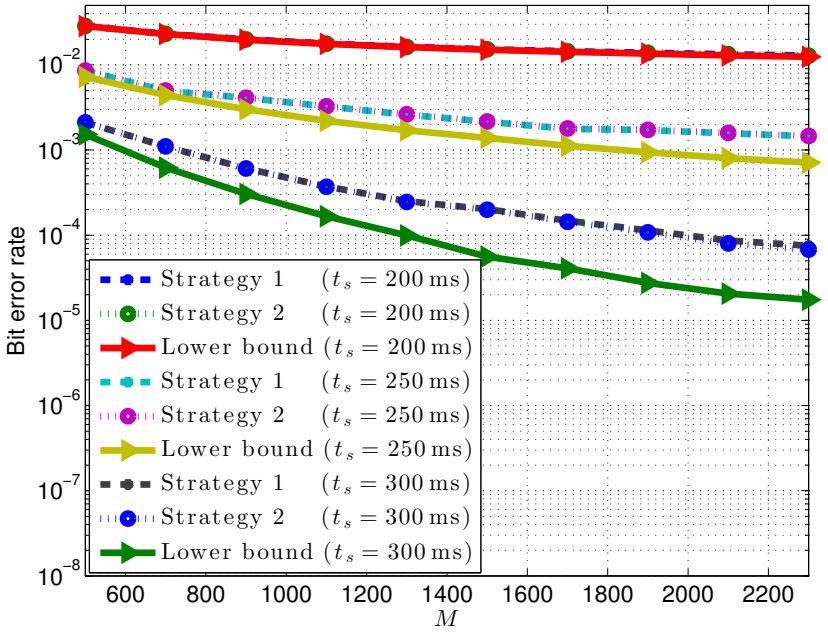

Figure 3.6. Comparison of bit error rates for the proposed strategies.

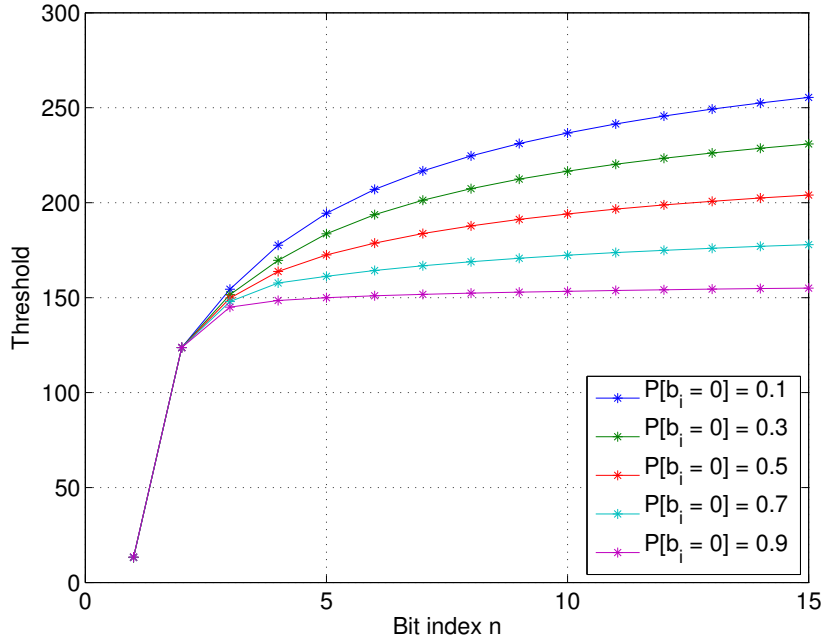

Figure 3.7. Optimal threshold values for different values of $P[b_i = 0]$, where $t_s = 200\,\text{ms}$ and $M = 1000$.

Additionally, rate of convergence depends on the value of $P[b_i = 0]$, since lower $P[b_i = 0]$ values yield a slower convergence due to the permanently increasing number of accumulating molecules. Curves depending on the numerical values of $P[b_i = 0]$ are given in Figure 3.7.

3.2. Decision Feedback Filtering

In this section, we consider a new type of decision-feedback filter for a BCSK encoded sequence with a lower computational complexity than the MMSE equalizer proposed in [22]. Unlike the additive Gaussian noise, the variance of C_i is signal dependent, and equalizer tap coefficients must be updated for each sample based on previously detected bits with a feedback mechanism [22]. Each update requires solving the set of equations given in (30) in [22], which implies that the computational complexity of the equalizer increases as the number of equalizer taps increases. On the other hand, DFF introduced in this section has a computational complexity independent of the number of filter taps, but requires a larger number of memory elements in order to achieve the same BER with the MMSE filter. Additionally, another approach for detection with low computational complexity can be found in [23], which decreases the expected ISI from each observation before comparing with a threshold, rather than adjusting the threshold itself as in proposed DFF. Likewise, an ISI cancellation technique that utilizes decision feedback for compensating the effect of one previously demodulated symbol can be found in [24].

As mentioned in Section III, the number of candidate sequences $\mathbf{d}_1^{\{i,j\}}$ and $\mathbf{d}_0^{\{i,j\}}$ increases with powers of 2 as i increases. On the other hand, when $\hat{\mathbf{b}}^{i-1}$ is available to receiver, there are only two candidate sequences conditioned on bit-0 and bit-1, which are $\mathbf{d}_0^{\{i,j\}} = \{\hat{\mathbf{b}}^{i-1}, 0\}$ and $\mathbf{d}_1^{\{i,j\}} = \{\hat{\mathbf{b}}^{i-1}, 1\}$, respectively. $\mu_1^{\{i,j\}}$, $\mu_0^{\{i,j\}}$, $\sigma_0^{\{i,j\}}$, and $\sigma_1^{\{i,j\}}$ can be calculated using (3.4) and (3.6), and these parameters can be used to calculate $\gamma^{*\{i,j\}}$ via solving the quadratic equation given in (3.12). Consequently, by storing previously estimated bits at the receiver, $\gamma^{*\{i,j\}}$ for each i can be calculated in a signal dependent manner, assuming that the decisions are correct.

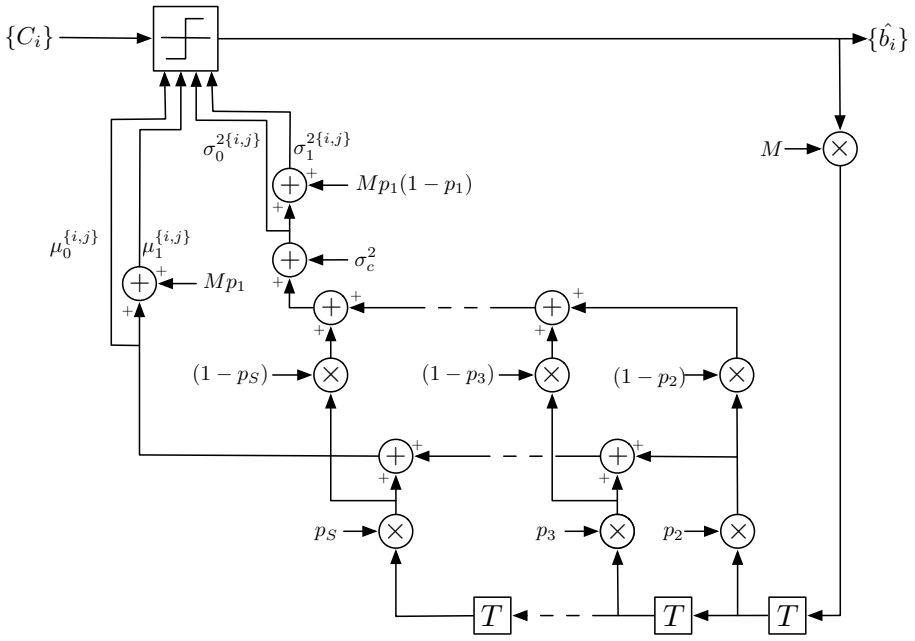

Figure 3.8. Block diagram of decision feedback filter.

In case of continuous transmission, storing $\hat{\mathbf{b}}^{i-1}$ for each i requires infinite memory, and is hence impractical. Rewriting distribution parameters for a finite memory receiver yields

$$\mu_0^{\{i,j\}} = M \sum_{k=2}^{S} p_k \, \hat{b}_{i-k+1}, \tag{3.26}$$

$$\mu_1^{\{i,j\}} = M \sum_{k=2}^{S} p_k \, \hat{b}_{i-k+1} + Mp_1, \tag{3.27}$$

$$\sigma_0^{2\{i,j\}} = \sigma_c^2 + M \sum_{k=2}^{S} p_k \, (1-p_k) \, \hat{b}_{i-k+1}, \tag{3.28}$$

$$\sigma_1^{2\{i,j\}} = \sigma_c^2 + M \sum_{k=2}^{S} p_k \, (1-p_k) \, \hat{b}_{i-k+1} + p_1 \, (1-p_1), \tag{3.29}$$

where S denotes the length of the receiver memory. Block diagram of this DFF is given in Figure 3.8. Note that the use of erroneously detected $\hat{\mathbf{b}}^{i-1}$ may cause error propagation, which may decrease the performance of the DFF.

Error performance of DFF and the MMSE equalizer proposed in [22] are compared via Monte Carlo simulations and bit error rates with respect to memory lengths

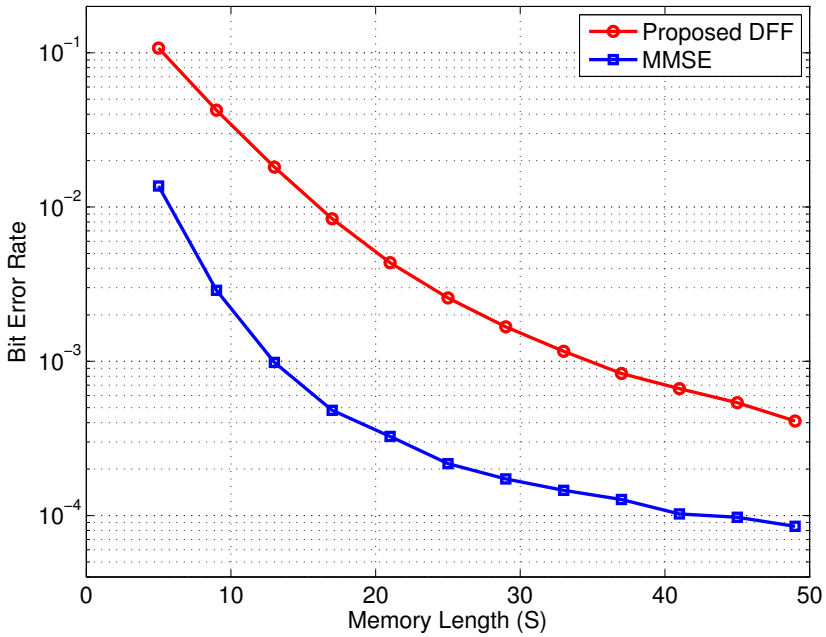

Figure 3.9. BER Curves for DFF and MMSE equalizer[2], where $M = 500$ and $t_s = 200\,\text{ms}$.

are given in Figure 3.9. BCSK modulation is employed for binary messages of length 1000 bits, and 500 realizations were performed in order to obtain an average.

As seen in Figure 3.9, in order for the DFF and the MMSE equalizer to perform at a bit error rate of around 10^{-3}, DFF must have $S = 35$, whereas $S = 13$ is sufficient for MMSE equalizer. However, if the computation of the distribution parameters are ignored, computational complexity of MMSE equalizer is at the order of $\mathcal{O}(S^3)$, whereas computational complexity of DFF is equal to $\mathcal{O}(S)$, since it only requires solving the quadratic equation given in (3.12). Note that variance of the received molecule counts depends on the transmitted message as given in (3.5), hence restricts the application of classical equalization methods.

[2]MMSE filter proposed in [22] stores $S = 2K - 1$ previously detected bits to calculate K equalizer taps.

Algorithm 1: Calculation of $\gamma^{*\{N\}}$

Compute $\gamma^{*\{1\}}$
for $i = 2$ to N **do**
  for $j = 0$ to $2^{i-1} - 1$ **do**
    Calculate $\{\mu_0^{\{i,j\}}, \mu_1^{\{i,j\}}, \sigma_0^{\{i,j\}}, \sigma_1^{\{i,j\}}\}$
    if $j = 2^{i-1} - 1$ **then**
      Compute optimal threshold $\gamma^{*\{i,2^{i-1}-1\}}$
      $\gamma_{max} \leftarrow \gamma^{*\{i,2^{i-1}-1\}}$
    end if
  end for
  Set step size $\rho = M/100$
  $\boldsymbol{\gamma} = \gamma^{*\{i-1\}} : \rho : \gamma_{max}$
  while $\rho > \zeta$ **do**
    Calculate the sum of likelihoods

$$\mathbf{r} = \frac{\sum_{j=0}^{2^{i-1}-1} P[b_i = 1]\mathcal{N}(\boldsymbol{\gamma}|\mu_1^{\{i,j\}}, \sigma_1^{\{i,j\}})}{\sum_{j=0}^{2^{i-1}-1} P[b_i = 0]\mathcal{N}(\boldsymbol{\gamma}|\mu_0^{\{i,j\}}, \sigma_0^{\{i,j\}})}$$

    $m^* \leftarrow \underset{m}{\operatorname{argmin}} |1 - r(m)|$
    $\gamma^{*\{i\}} \leftarrow \boldsymbol{\gamma}(m^*)$
    $\boldsymbol{\gamma} \leftarrow \gamma^{*\{i\}} - \rho : \rho/10 : \gamma^{*\{i\}} + \rho$
    $\rho \leftarrow \rho/10$
  end while
end for

Table 3.1. Distribution parameters.

Candidate Sequence	Mean	Standart Deviation	Probability of Occurance	Optimal Threshold
$\mathbf{d}_0^{\{2,0\}} = \{0,0\}$	$\mu_0^{\{2,0\}}$	$\sigma_0^{\{2,0\}}$	0.25	$\gamma^{*\{2,0\}}$
$\mathbf{d}_1^{\{2,0\}} = \{0,1\}$	$\mu_1^{\{2,0\}}$	$\sigma_1^{\{2,0\}}$	0.25	
$\mathbf{d}_0^{\{2,1\}} = \{1,0\}$	$\mu_0^{\{2,1\}}$	$\sigma_0^{\{2,1\}}$	0.25	$\gamma^{*\{2,0\}}$
$\mathbf{d}_1^{\{2,1\}} = \{1,1\}$	$\mu_1^{\{2,1\}}$	$\sigma_1^{\{2,1\}}$	0.25	

$\gamma^{*\{2\}}$

4. TRANSMITTER BASED ISI MITIGATION TECHNIQUES

In this section, two transmitter-based ISI mitigation techniques are proposed. The first technique is the molecular transition shift keying (MTSK), which is an energy efficient modulation technique that aims to decrease the detrimental effects of the ISI by utilizing two different molecule types. Second technique employs a power adjustment strategy by utilizing the residual molecules from the previous symbols, which is applicable for BCSK, BMoSK, and MTSK.

4.1. Molecular transition shift keying

In case of continuous transmission, the first bit-0 after a large number of consecutive bit-1s becomes hard to detect due to the ISI caused by the accumulated molecules in the channel. $\mathbf{b}^5 = \{1, 1, 1, 1, 0\}$ can be given as an example for such a case. It is hard for the decoder to detect b_5 due to the ISI caused by $\mathbf{b}^4$. This is the main motivation for MTSK, which aims to distinguish whether the number of received molecules C_i in the ith time slot is induced by the ISI due to $\mathbf{b}^{i-1}$, or a b_i being a 1, by decreasing the amount of ISI due to the residual molecules that belong to previous symbols.

As discussed in Section II, a proper choice of symbol duration allows us to sort the hitting probabilities in a descending order, such as $p_1 > p_2 > p_3 > ....$ The amount of decay between consecutive hitting probabilities also decreases decreasingly, which implies that most of the residual molecules that lead to ISI belong to the time slot immediately preceding the current one, and depends on the magnitude of p_2. Residual molecules from two or more previous time slots which are related to the magnitude of p_i for $i \geq 3$ have less significance. To visually illustrate this behavior, the hitting probabilities p_k for $k = 1, 2, ..., 10$ are given in Figure 4.1.

MTSK can be explained as follows. The bit-0s are encoded by the absence of the messenger molecules, and bit-1s are encoded by using two different types of molecules,

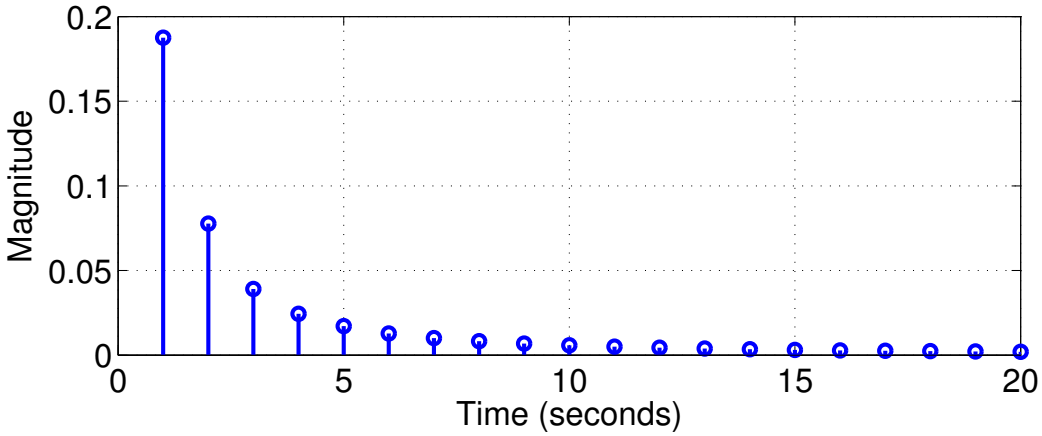

Figure 4.1. First 20 hitting probabilities, where $t_s = 200\,\text{ms}$.

denoted as type-A and type-B, of constant number of molecules, M, where the choice of the molecule type depends on the value of the following symbol in the message sequence. For the sake of simplicity, we assume that both molecule types have the same diffusion coefficient. type-A or type-B molecules are released for the next symbol values of bit-0 and bit-1, respectively. In case of CSK, bit-1s are encoded by emitting only type-A (or only type-B) molecules, which causes high amounts of ISI observed by bit-0s due to the accumulation of the same type of molecules in the channel. On the other hand, in case of MTSK, emitting type-B instead of type-A molecules before each bit-0 reduces the ISI induced by type-A molecules on each bit-0. Similarly, since type-B molecules are only emitted before a bit-0, their accumulation in the channel is less than the case where CSK is employed by emitting only type-B molecules. As a result, ISI observed by each bit-0 is decreased compared to the case where CSK is employed. An example sequence is given in Figure 4.2, where the modulated sequence is delayed for one symbol duration to obtain a causal representation, and $\mathbf{m}^n = \{m_1, m_2, ..., m_n\}$ represents the molecule types of the modulated message sequence that will be transmitted through the diffusion channel, where absence of messenger molecules is denoted with an "$\times$". This causal system can now be represented by the first-order Markov chain whose state transition diagram is given in Figure 4.3.

Since there are two types of molecules to be sensed in an MTSK modulated signal, a decision should be made based upon the information they jointly possess. Consequently, decoding an MTSK modulated signal requires an optimal choice of

$\mathbf{b}^{16}$:	0	1	1	1	0	1	0	1	1	0	1	0	0	1	1	0
$\mathbf{m}^{16}$:	×	A	A	B	×	B	×	A	B	×	B	×	×	A	B	×
Causal System :		×	A	A	B	×	B	×	A	B	×	B	×	×	A	B	×

Figure 4.2. MTSK modulated binary sequence example.

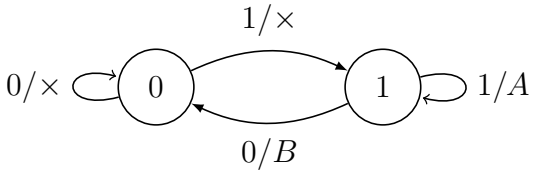

Figure 4.3. State diagram for MTSK encoder.

decision threshold for both molecule types. Since the receiver is assumed to detect both molecule types independently, $\mathbf{b}^n$ can be treated as two different messages; one modulated by using type-A and the other using type-B molecules, denoted as $\mathbf{b}^n(A)$ and $\mathbf{b}^n(B)$, respectively. $\mathbf{b}^n(A)$ and $\mathbf{b}^n(B)$ are illustrated in Figure 4.4 for the same $\mathbf{b}^{16}$ in Figure 4.2. Splitting $\mathbf{b}^n$ into $\mathbf{b}^n(A)$ and $\mathbf{b}^n(B)$ allows us to find optimal thresholds for each sequence, which are denoted by $\gamma_A^{*\{n\}}$ and $\gamma_B^{*\{n\}}$, respectively.

$\mathbf{b}^{16}(A)$:	0	1	1	0	0	0	0	1	0	0	0	0	0	1	0	0
$\mathbf{b}^{16}(B)$:	0	0	0	1	0	1	0	0	1	0	1	0	0	0	1	0

Figure 4.4. MTSK encoded binary sequence example.

Let $P_A[b_i = 1]$ and $P_B[b_i = 1]$ denote the probability of occurrence for 1 in $\mathbf{b}^n(A)$ and $\mathbf{b}^n(B)$, respectively. As given in (3.2), $\mathbf{b}^n(A)$ and $\mathbf{b}^n(B)$ can also be approximated as n independent Bernoulli trials with probabilities of success $P_A[b_i = 1]$ and $P_B[b_i = 1]$, respectively. Considering that each bit-1 run of length $r \geq 1$ in $\mathbf{b}^n$ contains exactly one bit encoded by molecule type-B, $P_B[b_i = 1]$ and $P_A[b_i = 1]$ can be calculated as

$$P_B[b_i = 1] = P[b_i = 1](1 - P[b_i = 1]), \tag{4.1}$$

$$P_A[b_i = 1] = P[b_i = 1] - P[b_i = 1](1 - P[b_i = 1]) = P[b_i = 1]^2, \tag{4.2}$$

$\gamma_A^{*\{i\}}$ and $\gamma_B^{*\{i\}}$ can therefore be determined by employing Algorithm 1 using the probabilities in (4.1) and (4.2), respectively.

Let $C_i(A)$ and $C_i(B)$ denote the number of received type-A and type-B molecules at the receiver due to the transmission of $\mathbf{b}^i(A)$ and $\mathbf{b}^i(B)$, respectively. Decision rule for each molecule type can be given as

$$C_i(A) \underset{\hat{b}_i(A)=0}{\overset{\hat{b}_i(A)=1}{\gtrless}} \gamma_A^{*\{i\}},$$

$$C_i(B) \underset{\hat{b}_i(B)=0}{\overset{\hat{b}_i(B)=1}{\gtrless}} \gamma_B^{*\{i\}},$$

where $\hat{b}_i(A)$ and $\hat{b}_i(B)$ denote the estimation of $b_i(A)$ and $b_i(B)$, respectively. To decide for a bit-0, both $\hat{b}_i(A) = 0$ and $\hat{b}_i(B) = 0$ must be satisfied. On the other hand, if at least one of the number of received molecules exceeds its corresponding threshold regardless of its molecule type, the decoder decides for a bit-1. Consequently, the decision rule for an MTSK encoded binary sequence can be given as

$$\hat{b}_i = \begin{cases} 1, & \text{if } C_i(A) > \gamma_A^{*\{i\}} \text{or } C_i(B) > \gamma_B^{*\{i\}}, \\ 0, & \text{if } C_i(A) \leq \gamma_A^{*\{i\}} \text{and } C_i(B) \leq \gamma_B^{*\{i\}}. \end{cases} \tag{4.3}$$

Example 4.1. *Consider a random binary sequence* $\mathbf{b}^3 = \{1, 1, 0\}$*, where* $P[b_i = 0] = 0.5$*,* $t_s = 200\,ms$ *and* $M = 100$*. To compare the error performance of the BCSK, BMoSK, and MTSK, probability of an erroneous decision for* b_3 *will be used, since ISI observed by* b_3 *due to previous bits being bit-*1 *makes it harder to decode.*

Calculating hitting probabilities for these parameters yields $\{p_1, p_2\} = \{0.1875, 0.0777\}$*. Using these probabilities, the parameters with their corresponding sequences and thresh-*

old values (calculated via Algorithm 1) are given in Table 4.1. Additionally, the decision rule for the BMoSK encoded sequences does not employ a threshold value and it can be expressed as

$$C_i(A) \underset{\hat{b}_i=0}{\overset{\hat{b}_i=1}{\gtrless}} C_i(B), \tag{4.4}$$

*since bit-*1 *is encoded by molecule type-A and bit-*0 *is encoded by molecule type-B.*

Table 4.1. Parameters for BCSK, BMoSK, and MTSK modulation techniques.

Modulation type	Modulated sequences	Mean (molecules)	Variance (molecules^2)	Threshold (molecules)
BCSK	$\mathbf{b}^3 = \{1,1,0\}$	$\mu_0^{\{3,3\}} = 11.68$	$\sigma_0^{2\{3,3\}} = 11.92$	$\gamma^{*\{3\}} = 14.64$
BMoSK	$\mathbf{b}^3(A) = \{1,1,0\}$	$\mu_0^{\{3,3\}}(A) = 11.68$	$\sigma_0^{2\{3,3\}}(A) = 11.92$	–
	$\mathbf{b}^3(B) = \{0,0,1\}$	$\mu_1^{\{3,0\}}(B) = 18.75$	$\sigma_1^{2\{3,0\}}(B) = 16.23$	–
MTSK	$\mathbf{b}^3(A) = \{1,0,0\}$	$\mu_0^{\{3,1\}}(A) = 3.90$	$\sigma_0^{2\{3,1\}}(A) = 4.75$	$\gamma_A^{*\{3\}} = 10.42$
	$\mathbf{b}^3(B) = \{0,1,0\}$	$\mu_0^{\{3,2\}}(B) = 7.77$	$\sigma_0^{2\{3,2\}}(B) = 8.17$	$\gamma_B^{*\{3\}} = 15.12$

Let $P_e^{BCSK}(b_i)$, $P_e^{BMoSK}(b_i)$, and $P_e^{MTSK}(b_i)$ denote the probabilities of error in the detection of b_i for BCSK, BMoSK, and MTSK modulated messages, respectively. These probabilities can be calculated as

$$P_e^{BCSK}(b_3) = P[C_3 > \gamma^{*\{3\}}] = Q\left(\frac{\gamma^{*\{3\}} - \mu_0^{\{3,3\}}}{\sigma_0^{\{3,3\}}}\right) = 0.1950,$$

$$\begin{aligned} P_e^{BMoSK}(b_3) &= P[C_3(B) > C_3(A)] = P[C_3(B) - C_3(A) > 0] \\ &= Q\left(\frac{\mu_1^{\{3,0\}}(B) - \mu_0^{\{3,3\}}(A)}{\sqrt{(\sigma_0^{\{3,3\}}(A))^2 + (\sigma_1^{\{3,0\}}(B))^2}}\right) = 0.0913, \end{aligned}$$

$$\begin{aligned} P_e^{MTSK}(b_3) &= 1 - P[C_3(A) < \gamma_A^{*\{3\}}]P[C_3(B) < \gamma_B^{*\{3\}}] \\ &= 1 - \left[1 - Q\left(\frac{\gamma_A^{*\{3\}} - \mu_0^{\{3,1\}}(A)}{\sigma_0^{\{3,1\}}(A)}\right)\right]\left[1 - Q\left(\frac{\gamma_B^{*\{3\}} - \mu_0^{\{3,2\}}(B)}{\sigma_0^{\{3,2\}}(B)}\right)\right] = 0.0064. \end{aligned}$$

As a result, $P_e^{BCSK}(b_3) > P_e^{BMoSK}(b_3) > P_e^{MTSK}(b_3)$*. Note that even though there are only two bit-*1*s before* b_3*, differences between error probabilities are noteworthy.*

In order to compare the error performance of BCSK, BMoSK, and MTSK, average signal power per symbol for these techniques must be defined. For BCSK, where $M_i = 0$ for $b_i = 0$, and $M_i = M$ for $b_i = 1$, average power per symbol can be defined as $\bar{P} = MP[b_i = 1]$. This is also valid for MTSK, since bit-1s are encoded with a constant number of M molecules, and bit-0s are encoded by the absence of molecules, independent of the molecule type. On the other hand, since BMoSK utilizes M number of molecules for both bit-0 and bit-1, average signal power of BMoSK will be equal to M. Error performance of the BCSK, BMoSK, and MTSK modulation techniques are compared via Monte Carlo simulations, and the resulting BER curves are given in Figure 4.5. Binary sequences of length 1000 were used, 10^4 realizations were performed, and threshold values computed via Algorithm 1 are employed in the simulations. As seen in Figure 4.5, error rates are significantly decreased when MTSK is employed. By comparison with BCSK, employing MTSK increases the system complexity, since it utilizes two different types of molecules instead of one. On the other hand, if utilization of two different molecule types is allowed, one can easily prefer MTSK over BMoSK, since the improvement in the communication quality is very significant. Furthermore, although both BMoSK and MTSK utilize two different types of molecules, employing BMoSK requires the transmitter to release molecules for both bit-0 and bit-1, whereas employing MTSK requires the release of molecules only for a bit-1. Thus, MTSK has an energy advantage.

4.2. Power Adjustment

Effects of ISI can both be beneficial (constructive interference) and harmful (destructive interference) to the symbol in question. In BCSK, BMoSK, and MTSK, residual molecules become a source of destructive interference when the intended symbol is a bit-0. On the other hand, they may actually be beneficial for consecutive bit-1s in a sequence and may be used to support the messenger molecules that will

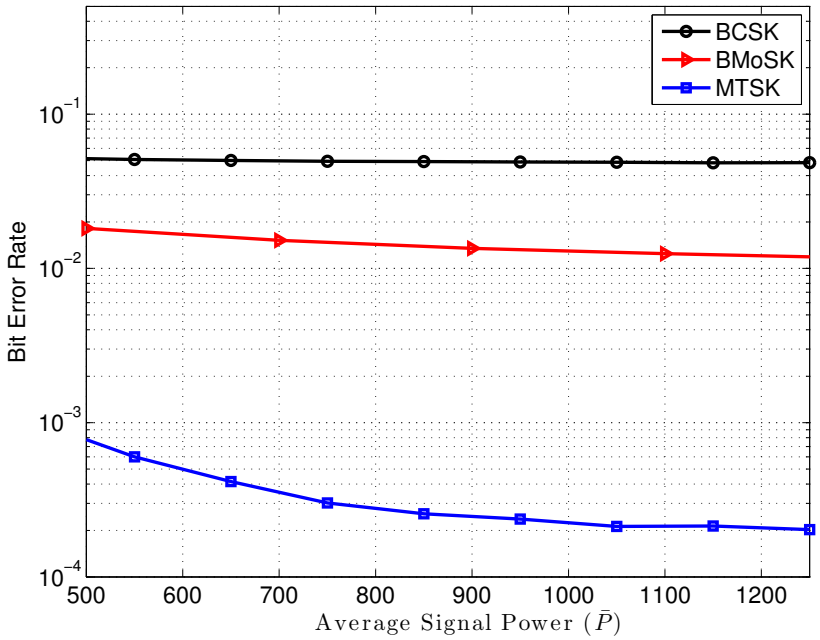

Figure 4.5. BER Curves for different modulation techniques, where $t_s = 200\,\text{ms}$.

be emitted in the next time slots. With this motivation, BCSK, BMoSK, and MTSK were modified to utilize the residual molecules from the previous symbols, and modified versions are denoted by BCSK-PA, BMoSK-PA, and MTSK-PA, where PA stands for power adjustment. A similar approach on utilizing residual molecules in terms of symbol duration adjustments can be found in [25]. Briefly, in [25], authors propose a dynamic structure at the receiver side, where they dynamically increase the symbol duration as the number of accumulated molecules increase in the channel. This helps preventing ISI.

Recall that, in case of a BCSK modulated signal, $M_i = 0$ for $b_i = 0$ and $M_i = M$ for $b_i = 1$. Since BCSK-PA intends to adjust the signal power considering the effects of constructive ISI, in case of a BCSK-PA modulated signal, value of M will be adjusted depending on the number of residual molecules in the channel.

Let $E[M_{REC}]$ denote the expected value of the received number of molecules at the receiver by sending M number of molecules for the first bit-1 in $\mathbf{b}^i$. Since $M_i = 0$ for $b_i = 0$, bit-0s before the first bit-1 in $\mathbf{b}^i$ will not effect the number of molecules

accumulated in the channel. Relationship between $E[M_{REC}]$ and M is given as

$$E[M_{REC}] = p_1 M. \tag{4.5}$$

For correct transmission, the threshold at the receiver side should be chosen so that $E[M_{REC}]$ number of molecules leads to a symbol decision of bit-1. For a sequence containing consecutive bit-1s, sending the same amount of molecules for each symbol increases the cumulative number of received molecules at the receiver side, exceeding $E[M_{REC}]$. This will also cause more molecules to accumulate in the channel and become a source of ISI for the following bit-0s. On the other hand, for the second and latter symbols, by sending a smaller number of molecules and making use of the residual ones from the previous time slots, $E[M_{REC}]$ can still be induced at the receiver and the intended symbol can be decoded correctly. This guarantees the accumulation of fewer molecules in the channel, which, in turn, reduces the amount of ISI for the following symbols. Number of molecules required to maintain $E[M_{REC}]$ number of molecules at the receiver after the transmission of the first bit-1 can be calculated as

$$M_i = E[M_{REC}] - E[M_i^R], \tag{4.6}$$

where $E[M_i^R]$ denotes the expected value of the residual molecules accumulated in the channel due to the transmission of $\mathbf{b}^{i-1}$. Since the channel is assumed to be free of messenger molecules before the transmission begins, $E[M_i^R]$ can be calculated as

$$E[M_i^R] = \sum_{j=2}^{i} p_j M_{i-j+1}. \tag{4.7}$$

Continuously calculating the effects of a large number of symbols from previous time slots is impractical. It is also possible to adjust M_i by using a finite memory of

length K, and rewrite (4.7) as

$$E[M_i^R] = \sum_{j=2}^{K} p_j M_{i-j+1}. \tag{4.8}$$

In order to apply power adjustment to BMoSK and MTSK modulated signals, expected value of the number of residual molecules must be calculated for both types of molecules, which are denoted by $E[M_i^R(A)]$ and $E[M_i^R(B)]$ for type-A and type-B molecules, respectively. Splitting $\mathbf{b}^i$ into $\mathbf{b}^i(A)$ and $\mathbf{b}^i(B)$ as was done in Figure 4.4 allows us to calculate $E[M_i^R(A)]$ and $E[M_i^R(B)]$ separately.

The power adjustment technique aims to maintain a constant number of received molecules for a bit-1, but by doing so, number of received molecules for a bit-0 fluctuates depending on K, and distorts the monotonically increasing behavior of optimal threshold values. Consequently, $\gamma^{*(i)}$ cannot be calculated for large i, and empirically found threshold values are used in the simulations.

Error performance of the BCSK-PA, BMoSK-PA, and MTSK-PA were compared via Monte Carlo simulations and BER curves for $K = 2$ and $K = 4$ are given in Figure 4.6 and 4.7, respectively. 15000 realizations were performed in order to obtain an average, and average power $\bar{P}$ is calculated by averaging the number of molecules used per realization for each modulation. Note that employing power adjustment decreases the error rates for all modulation techniques significantly, compared to the Figure 4.5, where there is no power adjustment employed. Since MTSK was also proposed to mitigate ISI, marginal effect of MTSK decreases when it's combined with the power adjustment technique. As a result, when power adjustment is employed, error rates for MTSK-PA and BMoSK-PA differs slightly. Furthermore, since the effect of K previous bits are considered, as K increases, improvement in the communication quality also increases. On the other hand, increasing K introduces more memory to the system, which results in a trade off between memory length and communication quality.

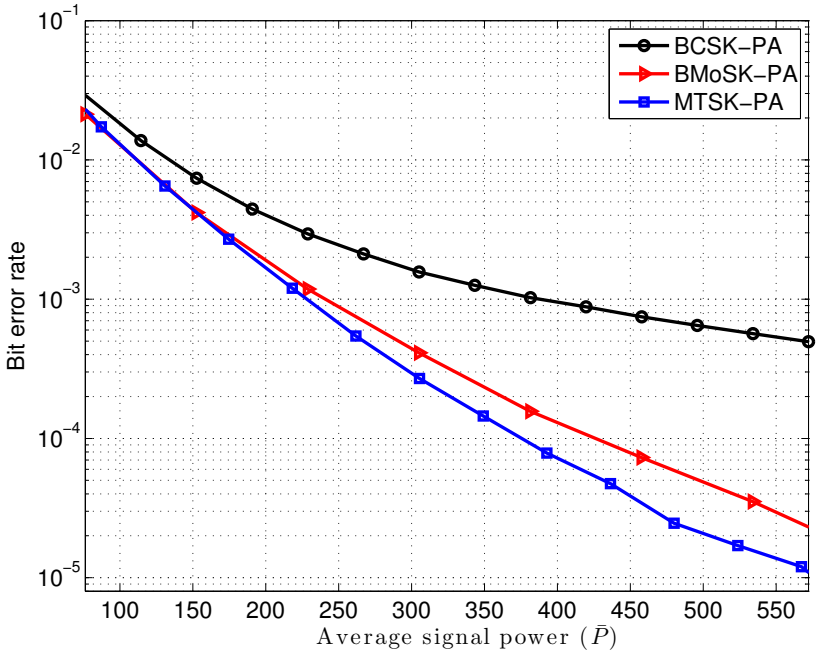

Figure 4.6. BER Curves for different modulation techniques with power adjustment for $K = 2$, where $t_s = 200\,\text{ms}$ and $P[b_i = 0] = 0.5$.

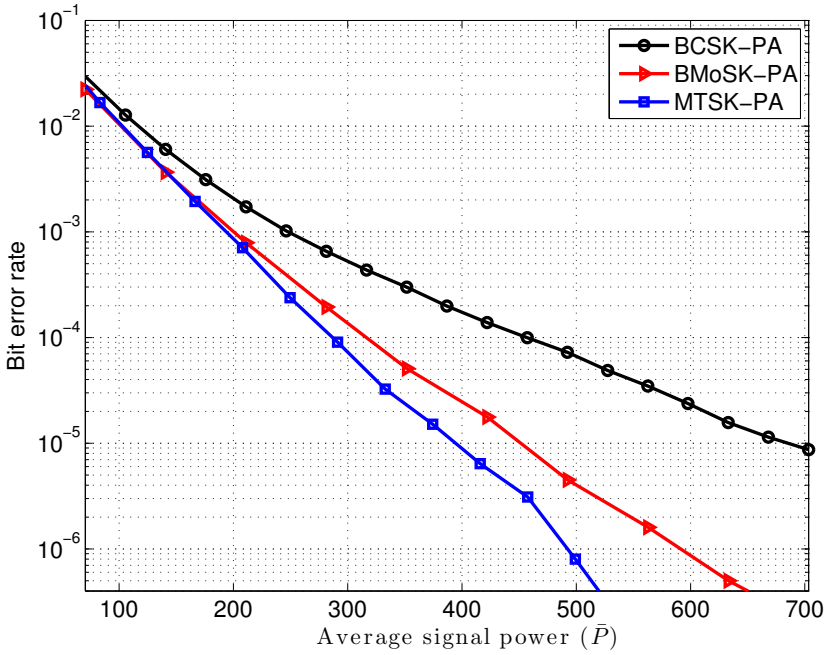

Figure 4.7. BER Curves for different modulation techniques with power adjustment for $K = 4$, where $t_s = 200\,\text{ms}$ and $P[b_i = 0] = 0.5$.

4.3. Pre-Equalization

As shown in Figure 2.2, due to the internal dynamics of the diffusion channel, the transmitted signal is transformed in the medium and the resulting received signal exhibits a shape that resembles a power-law function with a long tail, which causes intersymbol interference (ISI) and significantly reduces the system performance.

In the literature, several methods have been proposed to shape the received signal and mitigate the aforementioned shortcomings of the MCvD system. Inducing an impulse signal at the receiver side via deriving the inverse channel characteristics is proposed in [26]. Although this is a very elegant solution, the derived composite transmit pulse contains a negative element (poison signal), which is a continuous function of time. This means that the transmitter must *continuously* release *a varying* number of molecules into the communication medium. Furthermore, the poison signal is also a function of the distance between the transmitter and the receiver. This means that its amplitude will increase proportional to this distance. These factors, especially the fact that signal is continuous rather than discrete, makes the implementation of this mechanism very hard in a realistic environment. Another modulation technique, Zebra-CSK, for shaping the signal via using inhibitor molecules is proposed in [8]. While this method significantly reduces the ISI, its performance strongly relies on the inhibition efficiency, which is quite low in a 3-D liquid medium. Additionally, the symbol error probabilities are obtained considering the effect of only one previous symbol, not a continuous transmission. Another modulation technique, Molecular Concentration Shift Keying (MCSK), which utilizes two types of molecules for even and odd time slots, is proposed in [27].T his method also reduces ISI significantly, and is also implemented for a comparison with the proposed method.

In contrast to these works, in this paper, we consider a pre-equalization method in which the transmitter utilizes two types of MMs, type-A and type-B, and the receiver interprets the difference between the received quantities of these two types of molecules as the received signal. By doing so, the resulting received signal is shaped such that the interference is significantly reduced.

In order to distinguish how many and which type of molecules are emitted for a bit, let $M_0(x)$ and $M_1(x)$ denote the number of type-x molecules emitted for a bit-0 and bit-1, respectively. Considering the BCSK and BMoSK implementations, the MM emission strategy of both modulation techniques can be summarized as

- BCSK:
  - (i) $M_0(A)$: number of type-A molecules emitted for bit-0
  - (ii) $M_1(A)$: number of type-A molecules emitted for bit-1
  - (iii) $M_0(A)$ is generally chosen as $M_0(A) = 0$.
- BMoSK:
  - (i) $M_0(B)$: number of type-B molecules emitted for bit-0
  - (ii) $M_1(A)$: number of type-A molecules emitted for bit-1
  - (iii) $M_1(B) = M_0(A) = 0$.

Notice that $\mathrm{E}[C_i|\mathbf{b}^i]$ given in (3.4), which is frequently used in the literature [28], is indeed a discrete convolution, and can be used to derive the coefficients of the FIR filter that models the diffusion channel. Let h_k denote the coefficients of this FIR filter of length K, which can be calculated as

$$h_k = M_1(A)p_k \quad \text{for} \quad k = 1, 2, ..., K. \tag{4.9}$$

In order to quantify the amount of ISI in terms of channel coefficients, a signal-to-interference (SIR) measure is defined as

$$\mathrm{SIR} = \frac{h_1}{\sum_{k=2}^{K}|h_k|}. \tag{4.10}$$

At high data rates, i.e., when t_s is small, SIR decreases significantly due to the high amount ISI in the diffusion channel, hence the communication quality is

significantly reduced. The pre-equalization method proposed in this section aims to increase the SIR, thus allow higher communication quality with high data rates.

If equalization at the receiver side is intended, it must be employed in an adaptive manner, since the variance of the received signal varies with i, as in (3.4). Examples of receiver side equalizers can be found in [22], including minimum mean squared error (MMSE) or decision feedback equalizers (DFE), where the equalizer taps are updated for each sample. These equalizers employ complex operations which makes them inefficient in terms of energy and computational complexity.

Equalization can also be performed at the transmitter side by sending a secondary signal that will interfere with the primary signal destructively to reduce the ISI. Since negative molecules do not exist, destructive interference can be imitated by employing a subtraction operation at the receiver side. In order for the receiver to distinguish the primary signal from the secondary one, different types of molecules must be utilized.

In the case of BCSK, if $M_0(A) = 0$, the primary signal is formed of the type-A molecules sent for each bit-1. On average, $p_1 M_1(A)$ of these molecules out of $M_1(A)$ hit the receiver in the first time slot, and the residual ones cause ISI. In order to reduce the effects of ISI, a second type of molecule (type-B) can be sent for each bit-1, which targets the residual type-A molecules in the channel. This can be achieved by emitting type-B molecules with some delay after type-A molecules are emitted, and subtracting the number of received type-B molecules from the number of received type-A molecules at the receiver at each time slot. *This subtraction operation imitates the destructive interference between the primary and the secondary signals.*

Since the receiver performs a subtraction operation, the received signal can be defined as the difference between two random variables as $C_i = C_i(A) - C_i(B)$, where $C_i(A)$ and $C_i(B)$ denote the number of received type-A and type-B molecules, respectively.

Hitting probabilities for type-A and type-B molecules can then be defined as

$$p_k(A) = F_{\text{hit}}(kt_s) - F_{\text{hit}}([k-1]t_s), \tag{4.11}$$

$$p_k(B) = F_{\text{hit}}(kt_s - \tau) - F_{\text{hit}}([k-1]t_s - \tau), \tag{4.12}$$

where τ denotes the amount of delay that type-B molecules encounter.

It is important to note that $C_i(A)$ and $C_i(B)$ do not contain any information individually whereas their difference, $C_i = C_i(A) - C_i(B)$, constitutes the received signal. After the subtraction is performed, the receiver does not need to store $C_i(A)$ and $C_i(B)$ separately. Consequently, the resulting channel response can defined as

$$h_k = M_1(A)p_k(A) - M_1(B)p_k(B). \tag{4.13}$$

Channel responses before and after pre-equalization are illustrated in Figure 4.8. Note that SIR is significantly increased after pre-equalization is employed.

4.3.1. Optimizing the pre-equalizer parameters

In a classical communication scenario, one of the main objectives is to minimize the bit error rate (BER) subject to the constraint that the signal has an average power of $\bar{P}$. For BCSK with $M_0(A) = 0$, the average power per symbol can be defined as $\bar{P} = M_1(A)P[b_i = 1]$. This constraint must also be satisfied for the proposed pre-equalization method, such that $\bar{P} = M_1(A)P[b_i = 1] + M_1(B)P[b_i = 1]$, indicating that the average power per symbol must be portioned out between the primary and the secondary signals. Let α denote the fraction of the average signal power dedicated to the primary signal, such that $M_1(A) = \alpha\bar{P}/P[b_i = 1]$, and $M_1(B) = (1-\alpha)\bar{P}/P[b_i = 1]$. Rewriting SIR explicitly by using (4.13) leads to

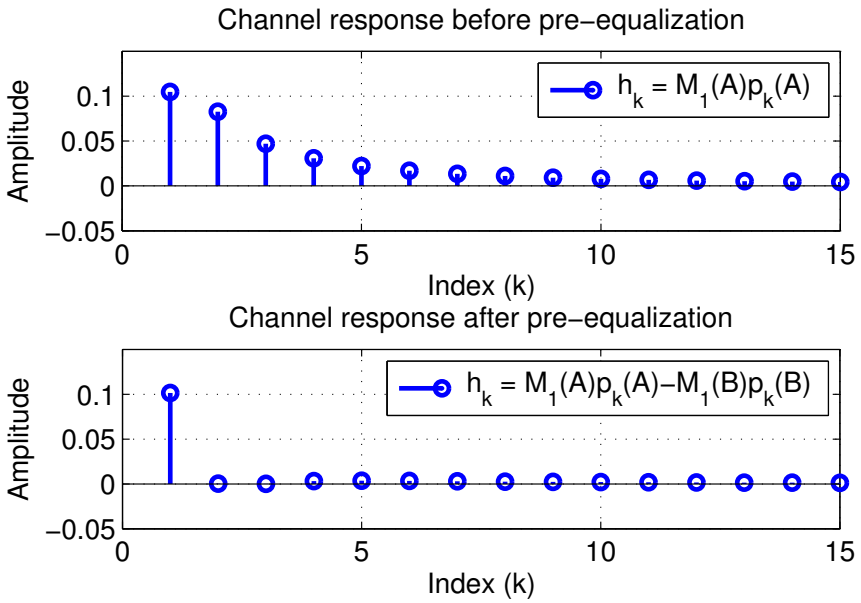

Figure 4.8. Channel responses before and after pre-equalization for $t_s = 100ms$, $\tau = 76ms$, $M_1(A) = 100$, and $M_1(B) = 66$.

$$\text{SIR} = \frac{\alpha(p_1(A) + p_1(B)) - p_1(B)}{\sum_{k=2}^{K} |\alpha(p_k(A) + p_k(B)) - p_k(B)|}, \tag{4.14}$$

which indicates that the amount of SIR for the proposed method is a function of τ and α. Since it is desirable to have the SIR as large as possible, optimal values for τ and α, τ^* and α^*, can be calculated by maximizing the SIR subject to the constraint that the signal has an average power of $\bar{P}$.

In order to calculate τ^* and α^*, derivative of (4.14) with respect to τ and α should be set to zero and should be solved simultaneously. For $K > 2$, this calculation becomes intractable due to the increasing number of additive terms in the denominator, hence the optimal values cannot be calculated analytically. In order to show that there exists a global maximum, heuristic techniques are used for various numbers of parameter sets. Heat map of SIR utilizing $K = 3$ for a given parameter set is presented in Figure 4.9.

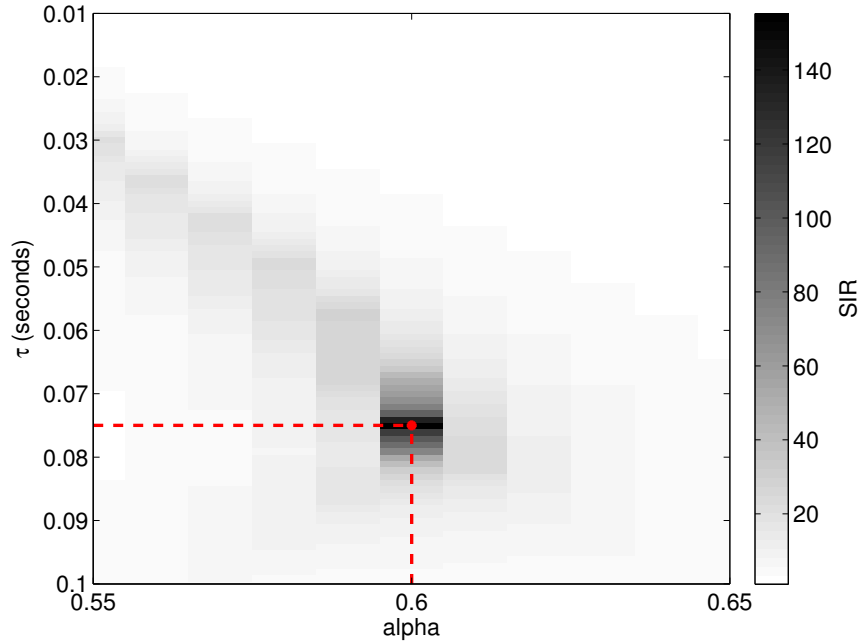

Figure 4.9. SIR for different τ and α values where $t_s = 100ms$, $K = 3$, $P[b_i = 0] = 0.5$, $r_r = 5\mu m$, $r_0 = 10\mu m$, and $D = 79.4\mu m^2/s$.

As seen in Figure 4.9, there is a global maximum. Note that, for different values of t_s, this computer search must be repeated in order to find τ^* and α^*.

In order to evaluate the performance of the proposed method, Monte Carlo simulations are employed. Results for BCSK, BMoSK, MCSK proposed in [27] and 3-tap adaptive MMSE equalizer proposed in [22] are also included in the plots. Briefly, MCSK utilizes different types of molecules for odd and even time slots with the same signal power. BER curves for $t_s = 80ms$, $t_s = 100ms$, and $t_s = 150ms$ are given in Figures 4.10, 4.11, and 4.12, respectively. Note that the choice of symbol duration determines the channel coefficients, which depends on r_r, r_0, and D. Environmental noise is assumed to have $\mu_0 = 2$, and systems parameters are chosen as $P[b_i = 0] = 0.5$, $r_r = 5\mu m$, $r_0 = 10\mu m$, and $D = 79.4\mu m^2/s$. Binary messages of length 10^2 bits are employed and 10^5 replications are performed in order to obtain an average. A maximum likelihood (ML) decoder is implemented for the receiver side for all modulation and equalization techniques.

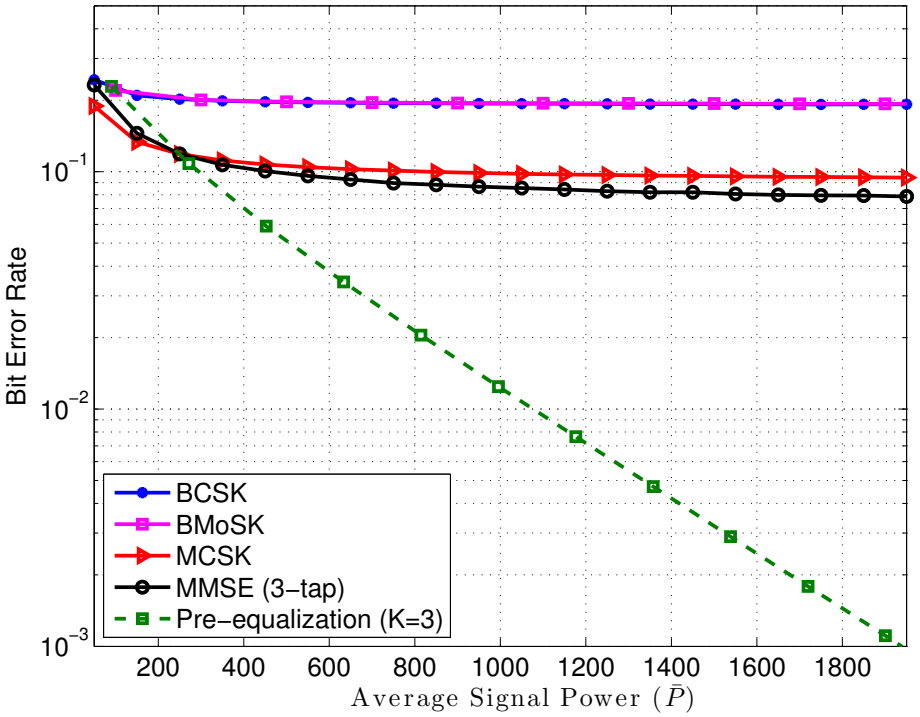

Figure 4.10. BER curves of BCSK, BMoSK, MCSK, MMSE and pre-equalization where $t_s = 80ms$.

As seen in Figures 4.10, 4.11 and 4.12, BER decreases significantly when pre-equalization is employed. Furthermore, due to the increasing SIR, error floor vanishes and error rate decreases very fast with increasing signal power. Notice that pre-equalization outperforms MCSK for higher data rates, whereas for higher symbol durations, MCSK outperforms the pre-equalization at small signal power values. On the other hand, although MCSK reduces ISI significantly, it will always lead to an error floor due to the residual molecules in the channel, unlike the proposed pre-equalization method. Furthermore, since the proposed method does not have an adaptive nature, it does not increase the system complexity compared to the other equalization techniques.

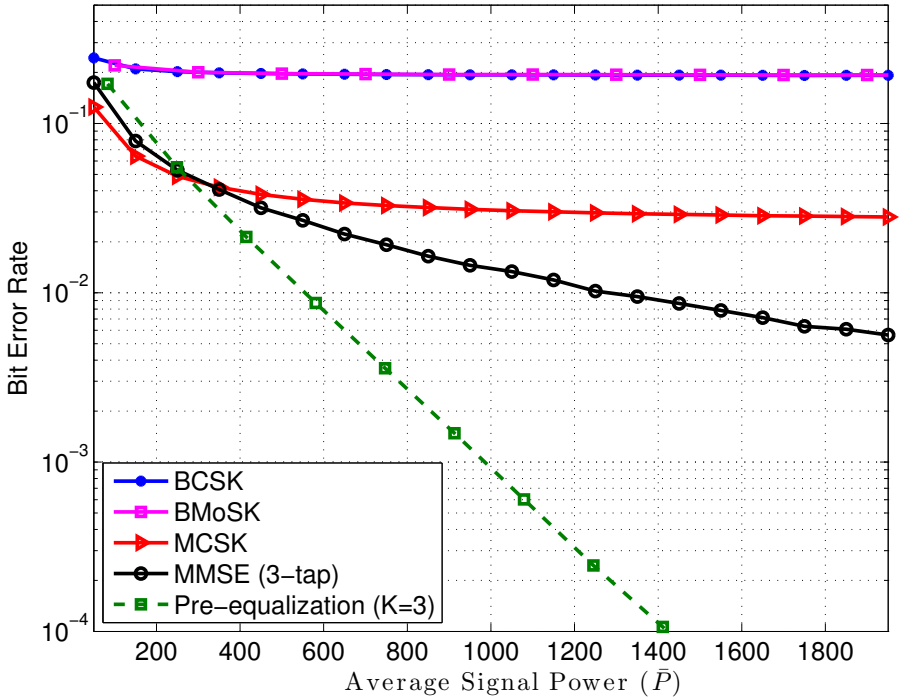

Figure 4.11. BER curves of BCSK, BMoSK, MCSK, MMSE and pre-equalization where $t_s = 100ms$.

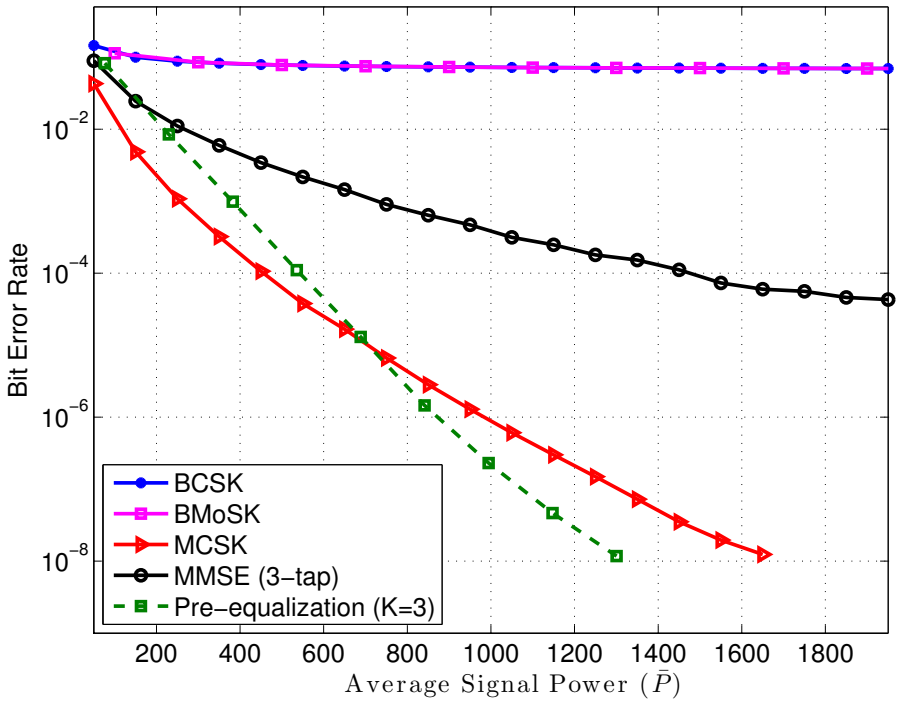

Figure 4.12. BER curves of BCSK, BMoSK, MCSK, MMSE and pre-equalization where $t_s = 150ms$.

5. CONCLUSIONS

In this thesis, transmitter and receiver based energy efficient ISI mitigation techniques are proposed for MCvD in terms of modulation, equalization, filtering, and signal power adjustment. To work on modulation techniques for a real time communication scenario, decision threshold for detection has to be determined prior to the information transmission, which is a problem never addressed in the literature before. As the first receiver based solution, an analytical method that minimizes the overall error rate with known system parameters is proposed to determine the optimal decision threshold for each symbol. Since the number of operations performed for calculating the optimal threshold increases for the latter symbols in the sequence, linear regression is applied to the first 25 threshold values, using a function that resembles the dynamics of the diffusion channel. By doing so, optimal thresholds can be calculated for each symbol regardless of the sequence length. These threshold values are compared with the empirical threshold values found via Monte Carlo simulations, and are verified to be optimal in the sense of minimizing the overall bit error rate. It is concluded that, as long as α_0, α_1, and β in (3.25) are known, different thresholding strategies can be applied depending on the system constraints. Resolving the thresholding problem is the pre-requisite step which allows us to propose new ISI mitigation techniques.

The second receiver-based solution proposed for the energy efficiency problem was to employ a simpler decoder in terms of computational complexity, titled decision feedback filter. DFF calculates the optimum threshold value for the symbol in question and updates the decision threshold for each sample by using the previously estimated bits. DFF was compared with the MMSE equalizer proposed in [22] in terms of bit error rate, memory length, and computational complexity via Monte Carlo simulations. It was concluded that DFF requires more memory to reach the same error rate as that of the MMSE equalizer, but since calculating the optimal threshold value has computational complexity at the order of $\mathcal{O}(S)$, DFF becomes more advantageous when energy efficiency is a priority.

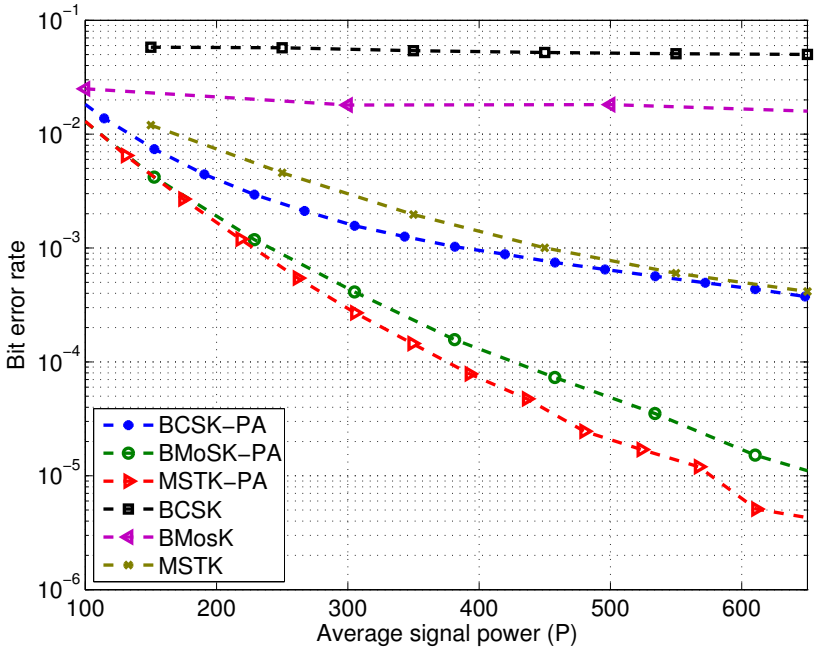

Figure 5.1. BER Curves for conventional and proposed modulation techniques, where $t_s = 200\,\text{ms}$.

The first transmitter-based solution proposed for ISI mitigation is a novel modulation technique, titled MTSK, which uses multiple molecule types in order to increase the data rate by suppressing the negative impact of the ISI on communication quality. It was shown via Monte Carlo simulations that MTSK decreases the bit error rates significantly, and outperforms the two most common modulation techniques in the literature, which are BCSK and BMoSK. Furthermore, as the second transmitter-based solution, a power adjustment technique, which uses residual molecules in the channel, is proposed to improve the energy efficiency. Error performance of BCSK-PA, BMoSK-PA, and MTSK-PA were compared via Monte Carlo simulations, and it was shown that the power adjustment technique decreases the ISI, hence the bit error rate for a fixed signal power for all modulation techniques, significantly. Furthermore, a trade off is observed between memory length (K) employed in PA and communication quality. In order to present a comprehensive comparison, bit error rates for all modulation techniques are presented in Figure 5.1.

As the third transmitter based solution, a pre-equalization method was proposed

to mitigate ISI for BCSK encoded sequences in a single-transmitter single-receiver MCvD system. The transmitter utilizes type-A and type-B molecules to modulate the primary and the secondary signals, respectively. Afterwards, the transmitter emits the secondary signal with a certain amount of delay, and the receiver performs a subtraction operation in order to imitate the destructive interference between the primary and the secondary signals. Optimal values for the amount of delay and secondary signal power are calculated numerically, and Monte Carlo simulations are employed to evaluate the system performance.

The proposed method decreases the interference, hence increases the SIR significantly. Furthermore, since the proposed method does not have an adaptive nature, it does not increase the system complexity compared to the other equalization techniques. We compare the proposed method with MCvD systems utilizing BCSK and BMoSK modulation as well as the MMSE equalizer and show that it significantly outperforms all of these methods, especially for high data rates.

As future work, more realistic models will be used in the simulations, rather than a point source transmitter and a spherical receiver. Moreover, rather than employing only binary symbols, quaternary symbols will also be considered, and modulation schemes will be expanded accordingly. Additionally, multiple transmitter multiple receiver systems can also be introduced, which will require new solutions to mitigate ISI.

REFERENCES

1. Akyildiz, I. F., F. Brunetti and C. Blázquez, "Nanonetworks: A New Communication Paradigm", *Computer Networks*, Vol. 52, No. 12, pp. 2260 – 2279, 2008.

2. Hiyama, S., Y. Moritani, T. Suda, R. Egashira, A. Enomoto, M. Moore and T. Nakano, "Molecular Communication", *NSTI Nanotechnology Conference*, Vol. 3, pp. 392–395, 2005.

3. Farsad, N., W. Guo and A. W. Eckford, "Tabletop Molecular Communication: Text Messages Through Chemical Signals", *PloS one*, Vol. 8, No. 12, p. e82935, 2013.

4. Nakano, T., A. W. Eckford and T. Haraguchi, *Molecular Communication*, Cambridge University Press, 2013.

5. Akyildiz, I. F., J. M. Jornet and M. Pierobon, "Nanonetworks: A New Frontier in Communications", *Commun. ACM*, Vol. 54, No. 11, pp. 84–89, 2011.

6. Nakano, T., M. Moore, F. Wei, A. Vasilakos and J. Shuai, "Molecular Communication and Networking: Opportunities and Challenges", *IEEE Transactions on NanoBioscience*, Vol. 11, No. 2, pp. 135–148, 2012.

7. Mahfuz, M., D. Makrakis and H. Mouftah, "On the Characterization of Binary Concentration-Encoded Molecular Communication in Nanonetworks", *Nano Communication Networks*, Vol. 1, No. 4, pp. 289–300, 2010.

8. Pudasaini, S., S. Shin and K. S. Kwak, "Robust Modulation Technique for Diffusion-based Molecular Communication in Nanonetworks", *CoRR*, Vol. abs/1401.3938, 2014.

9. Aijaz, A. and A.-H. Aghvami, "Error Performance of Diffusion-Based Molecular

Communication Using Pulse-Based Modulation", *IEEE Transactions on NanoBioscience*, Vol. 14, No. 1, pp. 146–151, 2015.

10. Kuran, M. S., H. B. Yilmaz, T. Tugcu and I. F. Akyildiz, "Modulation Techniques for Communication via Diffusion in Nanonetworks", *Proceedings of IEEE International Conference on Communications (ICC)*, pp. 1–5, 2011.

11. Kuran, M. S., H. B. Yilmaz, T. Tugcu and B. Özerman, "Energy Model for Communication via Diffusion in Nanonetworks", *Elsevier Nano Communication Networks*, Vol. 1, No. 2, pp. 86–95, 2010.

12. Jiang, C., Y. Chen and K. J. Ray, "Nanoscale Molecular Communication Networks: a Game-Theoretic Perspective", *EURASIP Journal on Advances in Signal Processing*, 2015.

13. Moore, M.-J., T. Suda and K. Oiwa, "Molecular Communication: Modeling Noise Effects on Information Rate", *IEEE Transactions on NanoBioscience*, Vol. 8, No. 2, pp. 169–180, 2009.

14. Saxton, M., "Modeling 2D and 3D Diffusion", A. Dopico (Editor), *Methods in Membrane Lipids*, Vol. 400 of *Methods in Molecular Biology*^{TM}, pp. 295–321, Humana Press, 2007.

15. Schulten, K. and I. Kosztin, "Lectures in theoretical biophysics", *University of Illinois*, Vol. 117, 2000.

16. Tyrrell, H. J. V. and K. R. Harris, *Diffusion in Liquids, A Theoretical and Experimental Study*, Butterworth Publishers, 1984.

17. Noel, A., K. C. Cheung and R. Schober, "Optimal Receiver Design for Diffusive Molecular Communication with Flow and Additive Noise", *IEEE Transactions on NanoBioscience*, Vol. 13, No. 3, pp. 350–362, 2014.

18. Mahfuz, M., D. Makrakis and H. Mouftah, "A Comprehensive Analysis of Strength-Based Optimum Signal Detection in Concentration-Encoded Molecular Communication with Spike Transmission", *NanoBioscience, IEEE Transactions on*, Vol. 14, No. 1, pp. 67–83, 2015.

19. ShahMohammadian, H., G. G. Messier and S. Magierowski, "Optimum Receiver for Molecule Shift Keying Modulation in Diffusion-Based Molecular Communication Channels", *Nano Communication Networks*, Vol. 3, No. 3, pp. 183 – 195, 2012.

20. Yilmaz, H. and C.-B. Chae, "Arrival Modelling for Molecular Communication via Diffusion", *Electronics Letters*, Vol. 50, No. 23, pp. 1667–1669, 2014.

21. Mohri, M., A. Rostamizadeh and A. Talwalkar, *Foundations of Machine Learning*, The MIT Press, 2012.

22. Kilinc, D. and O. Akan, "Receiver Design for Molecular Communication", *IEEE Journal on Selected Areas in Communications*, Vol. 31, No. 12, pp. 705–714, 2013.

23. Noel, A., K. C. Cheung and R. Schober, "Overcoming Noise and Multiuser Interference in Diffusive Molecular Communication", *Proceedings of ACM The First Annual International Conference on Nanoscale Computing and Communication*, pp. 1–9, ACM, 2014.

24. Yilmaz, H. B., N.-R. Kim and C.-B. Chae, "Effect of ISI Mitigation on Modulation Techniques in Molecular Communication via Diffusion", *Proceedings of ACM The First Annual International Conference on Nanoscale Computing and Communication*, NANOCOM' 14, pp. 3:1–3:9, ACM, New York, NY, USA, 2007.

25. Einolghozati, A., M. Sardari, A. Beirami and F. Fekri, "Capacity of Discrete Molecular Diffusion Channels", *IEEE International Symposium on Information Theory Proceedings (ISIT)*, pp. 723–727, 2011.

26. Wang, S., W. Guo and M. McDonnell, "Transmit Pulse Shaping for Molecular Communications", *Proceedings of IEEE Conference on Computer Communications Workshops*, pp. 209–210, 2014.

27. Arjmandi, H., A. Gohari, M. Kenari and F. Bateni, "Diffusion-Based Nanonetworking: A New Modulation Technique and Performance Analysis", *IEEE Communications Letters*, Vol. 17, No. 4, pp. 645–648, 2013.

28. Mosayebi, R., H. Arjmandi, A. Gohari, M. Nasiri-Kenari and U. Mitra, "Receivers for Diffusion-Based Molecular Communication: Exploiting Memory and Sampling Rate", *IEEE Journal on Selected Areas in Communications,*, Vol. 32, No. 12, pp. 2368–2380, 2014.